THEORY

Hybrid Quantum Noise Model to Compute Gaussian Quantum Channel Capacity

MOULI CHAKRABORTY [1], (Graduate Student Member, IEEE),
ANSHU MUKHERJEE [2], (Member, IEEE), **AVISHEK NAG** [3], (Senior Member, IEEE),
AND SUBHASH CHANDRA [1], (Member, IEEE)

[1] School of Natural Sciences, Trinity College Dublin, Dublin 2, D02 PN40 Ireland
[2] School of Electrical and Electronic Engineering, University College Dublin, Dublin 4, D04 V1W8 Ireland
[3] School of Computer Science, University College Dublin, Dublin 4, D04 V1W8 Ireland

Corresponding author: Mouli Chakraborty (chakrabm@tcd.ie)

ABSTRACT Quantum information processing leverages the principles of quantum mechanics, utilizing qubits, to improve computational and communicative tasks. In this realm, the quantum channel's capacity is pivotal in determining the efficiency and accuracy of quantum information handling, with its performance being significantly influenced by channel noise. Our study aims to establish a holistic hybrid quantum noise model to determine the quantum channel capacity. In this paper, we formulated a mathematical expression for this capacity and conducted simulations for both Gaussian and non-Gaussian inputs. A hybrid noise model is constructed by convolution of Poisson-distributed quantum noise with classical additive white Gaussian noise. We characterized the quantum-classical noise and the received signal using Gaussian Mixture Models. The maximum amount of quantum information that can be reliably transmitted over a quantum channel (per use of the channel) is determined by its capacity, and entropy and related quantities like mutual information play a role in calculating this capacity. Our formulation of quantum channel capacity is derived from the mutual information shared between the transmitter and receiver, encompassing the entropies of the signals. The quantum channel presents a higher capacity-to-signal-to-noise ratio for Gaussian inputs than non-Gaussian ones.

INDEX TERMS Quantum communication, statistical quantum signal processing, qubit, Gaussian quantum channel, quantum Poissonian noise, Gaussian noise, quantum Gaussian channel, Gaussian mixture models, quantum entropy, quantum channel capacity.

I. INTRODUCTION

Quantum communication is the science of transferring information using the principles of quantum mechanics, primarily employing quantum states of particles like photons for secure communication [1], [2], [3].

Quantum cryptography marks a significant advancement over traditional cryptographic methods. Quantum key distribution (QKD) is a method that ensures secure communication by allowing the detection of eavesdropping attempts using quantum principles such as superposition and entanglement [4]. Quantum key distribution (QKD) protocols, such as

BB84, exemplify this by using quantum properties to securely distribute encryption keys, making eavesdropping detectable due to the inherent nature of quantum states [1]. Quantum communication offers secure key exchange using quantum key distribution (QKD), utilizing the no-cloning theorem and properties such as photon polarization or phase [5], [6]. QKD, operational over hundreds of kilometers via optical fibers and quantum repeaters, detects eavesdropping and is superior to classical cryptography [7], [8]. Additionally, the scope of quantum communication extends beyond secure data transfer. It includes applications like quantum teleportation [9], which involves transferring quantum states between distant locations without the physical transfer of particles (qubits).

The associate editor coordinating the review of this manuscript and approving it for publication was Chi-Yuan Chen .

Quantum communication is crucial for the next generation of secure communications and holds a foundational and emerging component as quantum internet [10]. Continued progress in capabilities like quantum repeaters and memories could lead to large-scale quantum communication networks and a quantum internet [11]. The progress of Quantum Internet and quantum networks achieves full functionality through stages like trusted repeater development, entanglement distribution, and memory enhancement, culminating in seamless integration with the existing Internet, including management aspects [12]. In quantum networks, routing is an important problem, i.e., the problem of finding the shortest path in a network addressing the challenges of distributing quantum entanglement across a network of quantum repeaters with finite entangled qubit pairs and varying levels of entanglement fidelity [13]. Quantum sensing represents an advanced phase in integrated sensing, primarily focused on the trade-off between fundamental detection probability and achievable communication rates in communication systems [14].

Beyond security, quantum communication is foundational to the establishment of quantum networks, which are envisaged to interconnect quantum computers [10]. These networks, facilitating the sharing of quantum information (qubits) across distances, are essential for distributed quantum computing, enabling computational tasks that are currently impractical with classical networks. Integrating quantum communication with quantum information processing is critical for this technological evolution. Quantum gates and circuits play a crucial role in transforming classical information into quantum states that can be processed in a quantum information processing system more securely across quantum networks [1]. Quantum communication focuses on the transmission of quantum information, while quantum information processing involves the manipulation and processing of this information [15]. The synergy between these fields is expected to develop powerful quantum computing networks, mirroring the internet's role for classical computers today.

However, quantum communication, including quantum information processing, faces challenges, including developing reliable quantum repeaters for long-distance communication and managing quantum noise and decoherence. Efforts are also underway to integrate these quantum systems with existing infrastructure [2]. Despite these challenges, the continuous research in this domain promises substantial advancements in secure communication and the realization of global quantum networks and distributed quantum computing in the future.

Quantum noise, omnipresent in quantum computing, arises from various sources such as environmental interactions, qubit interactions, and imperfect controls, leading to errors like dephasing and decoherence. Characterizing and understanding its impact is challenging but crucial for practical quantum computation [16]. Classical and quantum noises are integral to a quantum channel's noise, with quantum noise often indistinguishable from classical noise in functional scenarios [17]. Noise from vibrations and material fluctuations interferes with communication signals, causing information loss. Both types of noise are essential in modeling noisy quantum channels, with classical communication often affected by thermal and shot noise. A standard model is the additive white Gaussian noise, which imitates random natural processes and can distort signal integrity, necessitating noise generators for system response measurement. Quantum Poisson noises can be considerable as follows: photon-counting shot noise [18], electron shot noise [19], quantum projection noise [20], quantum walk fluctuations [21], and more noises can be found in [22], [23], [24], and [25]. However, the classical noises that can be plugged into quantum noises are thermal noise [26], current shot noise [27], phase noise [28], amplifier noise [29], photodetector noise [30], and others ancillary noises are discussed in [31], [32], and [33].

Entanglement brings noise into the quantum communication channel. Entangled qubits decohere in noisy channels, losing entanglement through effects like sudden death [34]. Amplitude/phase damping also destroys correlations [35]. Furthermore, Gaussian states are vulnerable to thermal noise-adding photons [36], contaminating entanglement [37]. Quantum noise disturbs states, destroying information and entanglement through decoherence, dephasing, and photon loss. Decoherence can render channels useless by destroying information. The combined effect of these noises can severely affect the accuracy and performance of the quantum channel and overall quantum communication reliability. Decoherence can be linked to a form of "quantum noise" arising from interactions with the environment, causing errors and diminishing the reliability of quantum information in communication or computation [38]. Decoherence presents a formidable challenge in quantum communication, where accurate transmission and manipulation of quantum states are paramount.

Addressing decoherence in quantum communication is a crucial research effort. Several strategies and techniques are being developed to mitigate its effects [39], [40], [41], [42], [43]: Error correction codes and quantum error correction protocols are utilized to counteract the consequences of decoherence, protecting the delicate quantum information and improving the dependability and effectiveness of quantum communication systems [44]. Quantum error correction codes that utilize entanglement are being developed to approach the quantum capacity [45]. The paper [46] introduces a decoding method for quantum stabilizer codes using the GRAND technique from classical codes, applied to quantum BCH and polar codes. Reference [47] extends this to quantum-GRAND for quantum random linear codes, using quantum noise statistics for efficient error correction. Reference [48] compares classical and quantum error correction codes, detailing the construction of QECCs from classical
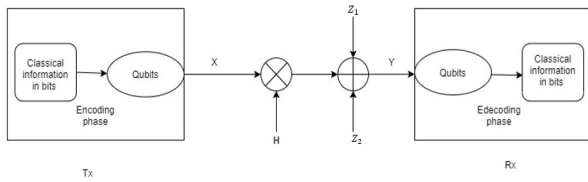
FIGURE 1. A noisy quantum channel model includes quantum noise Z_1 and classical noise Z_2 simultaneously under a single-channel link, the channel matrix $H = I$ is the identity matrix.

TABLE 1. Notation.

tr	The trace of a matrix
$T(\cdot)$	Trace-preserving map T
$A^\dagger$	The adjoint of A
A^t	The transpose of A
$\otimes$	The tensor product
$\mathcal{N}$	Gaussian density
$|\cdot\rangle$	The ket
$\langle\cdot|$	The bra

codes and their application to CSS and non-CSS codes. These works highlight the evolution of error correction methods in quantum computing, emphasizing adaptability and efficiency in handling quantum noise and error rates.

Matching ultrafast decoherence timescales with slower classical noise is challenging. Combining these mitigation strategies aims to improve robustness against decoherence in quantum communication. Approaches to match decoherence timescales: modeling via primary equations [49], high-bandwidth colored noise, phase/frequency jitter noise, discrete femtosecond noise injection [50], fast physical noise sources, modeling loss via short channel correlations [51]. Independent classical and quantum noise combines to a Gaussian distribution [52]. Adding equivalent sources such as shot noise preserves the power spectral density [53]. Uncorrelated noise sums in signal-to-noise ratio [54]. Correlated noise needs quantum treatment.

Combining classical and quantum noise poses challenges because of their distinct timescales. Numerical simulations with discrete time steps allow the concurrent influence of both types of noise [55]. Classical noise models employ analytical representations, while quantum noise uses Monte Carlo sampling [56] or Lindblad operators [57]. Independent noise sources in the primary / Langevin equations drive the evolution of the density matrix of the system [58], [59]. Classical parameters modulate the characteristics of quantum noise over time [15]. Decoherence must be considered, as it is a rapid quantum process causing entanglement with the environment and loss of quantum properties [38], [44].

This research developed a comprehensive hybrid noise model that combines the classical and quantum noises subsequently applied to estimate the capacity factor. It is considered a scenario of quantum communication where the sender and receiver are classical. We are more interested in the architecture when both sender and receiver use classical devices for communication, as it is a more practical scenario because of the limited availability of quantum computers. To avail quantum security in communication links, classical information is coded in quantum states (e.g., into the states of the photon); hence, the single quantum channel will be used to transport the quantum information. On the receiver side, the received signal in the form of quantum information will be delivered, and received quantum information will be decoded into the classical signal by measurement procedures. The maximum achievable data rate, that is, the classical capacity of a quantum channel, will be calculated through this process. On the other hand, there is another use case where the sender and receiver communicate with quantum devices, and the channel between them is purely quantum. In that case, the investigated channel capacity will be the quantum capacity of the quantum channel. The literature has reported [15] classical capacity of the quantum channel or quantum capacity of a quantum channel. For that capacity, expression is derived from the density matrices of qubit. However, the lack of the statistical formulation of the quantum channel has been spotted [60], and simulating results like how capacity varies to signal-to-noise ratio have been unavailable so far [15]. The lack of models for the probability distribution function of hybrid quantum noise and quantum received signals was another motivation behind this research Fig. 2 explains the direction of the research pictorially. The contributions of this paper are many-fold, involving introducing the statistical theory of the hybrid quantum noise model considering quantum Poissonian noise and classical additive white Gaussian noise (AWGN), hence the mathematical expression for the capacity of the Gaussian quantum channel. However, we worked on the Gaussian quantum channels, but they do not necessarily have Gaussian input. To compare these two cases, it is essential to vary the input distribution to determine how capacity will fluctuate with respect to the signal-to-noise ratio for the Gaussian and non-Gaussian input for the Gaussian quantum channel.

The main contributions of this paper are (I) Designing a noisy quantum channel via modeling hybrid quantum noise by considering it as a combination of quantum Poissonian noise and classical additive white Gaussian noise, (II) Proposed a closed-form solution for the capacity of Gaussian quantum channel despite of Gaussian Mixture (GM) Noise densities and GM output signal models, (III) Compare the results from the capacity tendency (the fluctuation of capacity or the growth / increasing/ decreasing nature of the capacity with respect to the signal-to-noise ration will be evaluated), for Gaussian and non-Gaussian inputs, (IV) The statistical interpretation of quantum channels has been introduced in this paper for the development of statistical quantum signal processing. It also analyzes the received signal models for Gaussian variate transmitted signal and non-Gaussian inputs for the Gaussian quantum channel. The model is studied in detail in the current article, and particular emphasis is paid when comparing capacities for Gaussian and non-Gaussian input for the quantum channel.
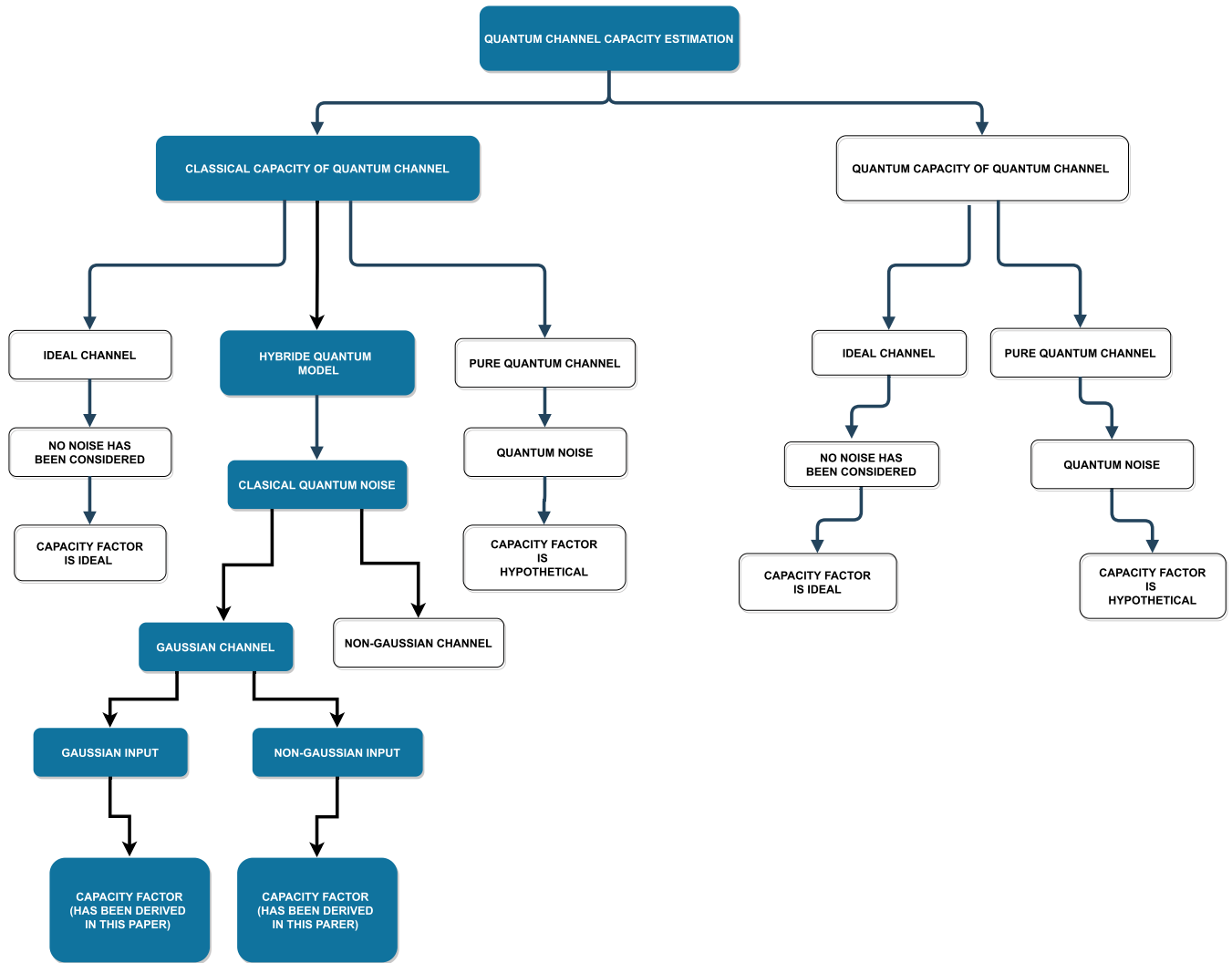
FIGURE 2. The categorization of noise and capacity factor of Gaussian quantum channel.

II. QUANTUM CHANNEL MODEL ANALYSIS

Quantum information processing (QIP) is based on quantum states for data manipulation [15]. Unlike classical information processing, which uses classical bits based on macroscopic properties, QIP employs quantum states with qubits as basic units. These qubits are represented by quantum state vectors, e.g., $|\psi\rangle = \alpha |0\rangle + \beta |1\rangle$, $\alpha, \beta \in \mathbb{C}$, reflecting their probabilistic nature, hinging on quantum phenomena like superposition and entanglement. Various physical systems can generate quantum states, with light consisting of photons ideal for long-distance communication. Entangled single- and two-photon states are desirable but challenging to prepare, making Gaussian states, such as coherent states [61], a more practical choice. Gaussian states, characterized by their Gaussian distribution in phase or Fock space, have proven to be robust for numerous QIP tasks. Quantum optical Gaussian states are pivotal in quantum information experiments, facilitating progress in bright and weak Gaussian light contexts. Extending discrete quantum

variables' theoretical and experimental successes to continuous variables is a compelling endeavor [37], [62]. Gaussian states are central to this exploration, given the enhanced capabilities of quantum optical systems [63], [64]. They underpin properties, entanglement theory, communication protocols, and emerging directions such as Gaussian cluster states for quantum computing [65], [66].

A. GAUSSIAN CHANNEL

In mathematical terms, a quantum channel is defined as a completely positive trace-preserving map $\rho \mapsto T(\rho)$ that takes states, i.e., density operators ρ acting on some Hilbert space $\mathcal{H}$, into states. This research assumed that output and input Hilbert spaces are identical for simplicity. Every channel can be conceived as a reduction of unitary evolution in a larger quantum system. So for any channel T there exists a state ρ_E on a Hilbert space $\mathcal{H}_E$, and a unitary U such that

$$T(\rho) = tr_E[U(\rho \otimes \rho_E)U^\dagger] \tag{1}$$

The system labeled E serves as an environment, embodying degrees of freedom, including observation, inducing a decoherence process. The channel is then a local manifestation of the unitary evolution of the joint system. A Gaussian channel [67], [68], [69], [70], [71] is now a channel of the form as in Eq.(1), where U is a Gaussian unitary, determined by a quadratic Bosonic Hamiltonian, and ρ_E is a Gaussian state [68]. This restriction to quadratic Hamiltonian gives a pretty good description of the physical system, such as the lossy optical fiber. In this study, the quantum channel is assumed to be Gaussian. However, the input states are not necessarily taken to be Gaussian.

The simplest Gaussian channel is a lossless unitary evolution governed by a quadratic Bosonic Hamiltonian:

$$\rho \mapsto U\rho U^{\dagger}, U = e^{i/2} \sum_{k,l} H_{kl} \mathcal{R}_k \mathcal{R}_l$$

with H being a real and symmetric $2n \times 2n$ matrix, $\mathcal{R}$ represents the canonical coordinates for the quantum system with n modes that is n canonical degrees of freedom [72], [73]. Such unitaries correspond to a representation of the real symplectic group $Sp(2n, \mathbb{R})$, formed by those real matrices for which $S\sigma S^t = \sigma$, where the matrix σ defines the symplectic scalar product [72], [73].

Such linear transformations preserve the commutation relations, the relation between such a canonical transformation in phase space and the corresponding unitary in Hilbert space is given by $S = e^{H\sigma}$. Gaussian unitaries are omnipresent in physics, particularly in optics, and this is the reason why Gaussian channels play such an important role. Notably, the action of ideal beam splitters, phase shifters, and squeezers correspond to symplectic transformations.

Depending on the context, it is appropriate or transparent to formulate a Gaussian channel in the Schrodinger picture $\rho \mapsto T_{A,Z}(\rho)$ or to define it as a transformation of covariance matrices

$$\gamma \mapsto A^t \gamma A + Z \qquad (2)$$

This is the most general form of a Gaussian channel. A serves the purpose of amplification, attenuation, and rotation in phase space, whereas the contribution Z is a noise term that may consist of quantum (required to make the mapped physical) and classical noise. Interestingly, A can be any real matrix, and therefore any map $\gamma \mapsto A^t \gamma A$ can be made approximately, as long as 'sufficient noise' is added [72], [73].

B. SYSTEM MODEL
According to (2), a single quantum link can be expressed as $\gamma \mapsto \gamma + Z$, where Z indicates the noise term consists of the quantum and the classical part. In (2), consider $A \mathcal{D} I$ as A can be any real matrix. The only condition of the map above being a quantum channel is to ensure sufficient noise is added [72], [73]. In terms of a mathematical equation, this unity quantum communication channel can be expressed as $Y = X + Z$, where X, Y, and Z

correspond to the random variables of the transmitted signal, received signal, and noise affecting the channel resulting from different unwanted sources, respectively. Since we consider a realistic quantum communication network carrying classical information, we assume the communication links suffer from classical and quantum noise components. We start with the assumption that the hybrid quantum-classical noise is additive in nature, such that $Z = Z_1 + Z_2$, where Z_1 is the Poisson distributed quantum shot noise and Z_2 is the Gaussian distributed white classical noise. More specifically, statistical modeling of the signals in statistical signal processing, this study develops similar techniques for statistical quantum signal processing to express the transmitted signal, the received signal, and the joint noise by random variables X, Y, and Z by the relation $Y = X + Z$ to find a distribution for the received signal. The same technique has been used to statistically showcase the joint quantum noise using the relation $Z = Z_1 + Z_2$. Figure 1 explains the theory in the schematic diagram.

III. METHODOLOGY
In this section, we will discuss a brief overview of the current research. Starting with the channel equation $Y = X + Z$, where X, Y, and Z correspond to the random variables of the transmitted signal, received signal, and hybrid quantum noise, the p.d.f. of the hybrid quantum noise will be the convolutional product of the component Quantum Poissonian noise and additive white Gaussian noise. This hybrid quantum noise model will be convoluted with the (I) Gaussian and (II) non-Gaussian input separately to get the received signal models of each setup. In the meantime, the entropies of received signals and the hybrid quantum noise will be calculated to evaluate (I) the mutual information between the Gaussian transmitted signal and the corresponding received signal, and (II) the mutual information between the non-Gaussian transmitted signal and the corresponding received signal. Finally, the capacity of the Gaussian channel will be calculated for (I) Gaussian and (II) non-Gaussian input separately to compare their trends to the signal-to-noise ratio. Fig. 3 explains the flow of the research methodology.

IV. QUANTUM NOISE MODEL
In terms of mathematics, the classical additive white Gaussian noise and quantum Poisson noise are jointly described as $Z = Z_1 + Z_2$, where Z_1 is the noise arising from quantum fluctuations that have a Poissonian distribution and Z_2 is the classical counterpart which has a Gaussian distribution. The statistical description of the hybrid classical-quantum noise Z is calculated considering it as a convolution product of Z_1 and Z_2.

Quantum noise Z_1 follows a Poisson distribution with parameters λ, and classical noise Z_2 follows a normal distribution with parameters μ_{Z_2} and σ_{Z_2}. Mathematically, $Z_1 \sim \mathcal{P}(\lambda), \lambda \geq 0, \lambda \in \{0, 1, 2, \ldots\}$ and $Z_2 \sim \mathcal{N}(\mu_{Z_2}, \sigma_{Z_2}^2)$ where μ_{Z_2} and $\sigma_{Z_2}^2$ are the mean and variance of the distribution, respectively. The quantum-classical noise
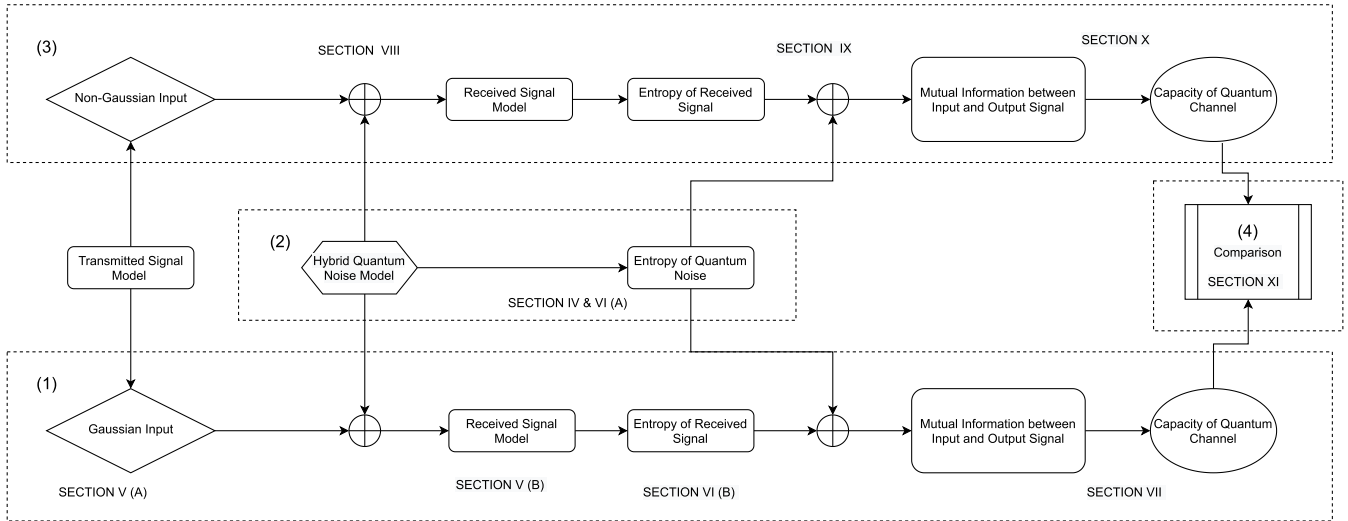
FIGURE 3. Flowchart of the research which is divided into four parts represented in the paper as follows: (1) Starting with the transmitted signal model with Gaussian inputs in Section V-A → Received signal model in Section V-B → The entropy of the received signal in Section VI-B → Mutual information b/w input and output signal → Capacity for the quantum channel in Section VII, (2) Section IV contains the hybrid quantum-classical noise model, and Section VI-A shows the entropy of the noise, (3) For non-Gaussian input, focus on Section VIII → Receive signal model → The entropy of the received signal in Section IX → Mutual information b/w input and output signal → Capacity for the quantum channel in Section X, (4) The comparison of capacities for the quantum channels with respect to signal-to-noise ratio has been shown in Section XI.

is modeled as a convolution product of Poisson and Gaussian distributions.

The probability mass function (p.m.f.) of Z_1 is given by,

$$f_{Z_1}(k) = \frac{e^{-\lambda}\lambda^k}{k!} \tag{3}$$

where $\lambda \geq 0$ and $k \in \{0, 1, 2, \ldots\}$

The probability density function (p.d.f.) of Z_2 can be expressed as,

$$f_{Z_2}(t) = \frac{1}{\sigma_{Z_2}\sqrt{2\pi}} e^{-\frac{1}{2}\left(\frac{t-\mu_{Z_2}}{\sigma_{Z_2}}\right)^2} \tag{4}$$

where μ_{Z_2} and σ_{Z_2} are the mean and standard deviation (s.d.) of the corresponding distribution.

Z_1 has a discrete distribution while Z_2 has a continuous distribution, but to develop the hybrid noise model, we need to calculate their joint distribution. This is done by expressing the p.m.f. of the discrete Poisson distribution in terms of the p.d.f. of a continuous distribution and then calculating the joint distribution of two continuous distributions.

The cumulative distribution function (c.d.f.) of the discrete r.v. Z_1 can be written as

$$F_{Z_1}(t) = \sum_{\forall k \in R_{Z_1}} P_{Z_1}(k)u(t - k) \tag{5}$$

where $R_{Z_1} = \{0, 1, 2, \ldots\}$. Now, the p.d.f. of the above function can be written as

$$f_{Z_1}(t) = \frac{dF_{Z_1}(t)}{dt} = \sum_{\forall k \in R_{Z_1}} P_{Z_1}(t)\frac{d}{dt}u(t - k)$$

$$= \sum_{\forall k \in R_{Z_1}} P_{Z_1}(t)\delta(t - k) = \sum_{\forall k \in R_{Z_1}} \frac{e^{-\lambda}\lambda^k}{k!}\delta(t - k) \tag{6}$$

where $\delta(x) = \frac{d}{dx}u(x)$ is the Dirac delta function and $u(\cdot)$ is the unit step function.

We know that if U is a discrete r.v. with p.m.f. $p_U : \chi \to [0, 1]$, and χ is a discrete set (maybe countably infinite), then the r.v. U can be thought of as a continuous r.v. with p.d.f.

$$f_U(u) = \sum_{\forall u_s \in \chi} p_U(u_s)\delta(u - u_s).$$

Now, if V is a continuous r.v., and $W = U + V$ is a hybrid r.v. then the p.d.f. of W can be computed from p.d.f.s of U and V. Assuming U and V are independent r.v.s, the p.d.f of W can be expressed as a convolution product of p.d.f.s f_U and f_V. Therefore,

$$f_W(w) = \sum_{\forall u_s \in \chi} p_U(u_s)f_V(w - u_s).$$

For our case, from the expressions (4) and (6) the p.d.f. of Z can be written as,

$$f_Z(z) = \sum_{\forall k \in R_{Z_1}} f_{Z_1}(k)f_{Z_2}(z - k)$$

$$= \sum_{k=0}^{\infty} \frac{e^{-\lambda}\lambda^k}{k!} \frac{1}{\sigma_{Z_2}\sqrt{2\pi}} e^{-\frac{1}{2}\left(\frac{z-k-\mu_{Z_2}}{\sigma_{Z_2}}\right)^2} \tag{7}$$

Hence, we evaluate the differential entropy of the r.v. Z given by the formula:

$$h(Z) = -\int_{\chi_Z} f_Z(z)\log_2 f_Z(z)\,dz$$

where χ_Z is the support of f_Z, i.e., the set on which f_Z is nonzero.

V. QUANTUM SIGNAL MODEL FOR GAUSSIAN INPUT

In quantum mechanics, a Fock state or number state is a quantum state that is an element of a Fock space with a well-defined number of particles (or quanta). These states are named after the Soviet physicist Vladimir Fock. In experimental practice, it is of general concern how robustly quantum states can be manipulated. A pure quantum state is symbolized by a ray in a Hilbert space over complex numbers [74]. However, density matrices can represent mixed states: positive semi-definite operators that act on Hilbert spaces [75]. In practice, the preparation of single-photon or two-photon entangled states (deterministically) is complex. Single-photon sources are light sources that can emit light as single particles or photons. They are distinct from coherent light sources (e.g., lasers) and thermal light sources (incandescent light bulbs). The Heisenberg uncertainty principle conveys that a state with an exact number of photons of a single frequency cannot be created. However, the Fock states or number states can be observed for a system where the amplitude of the electric field is distributed over a narrow bandwidth. Fock states play an important role in the second quantization formulation of quantum mechanics. In these circumstances, a single-photon source rises to an effectively one-photon-number state. Photons from an ideal single-photon source manifest quantum mechanical characteristics.

A. QUANTUM TRANSMITTED SIGNAL MODEL

Mathematically, a state is Gaussian if its distribution function in phase or its density operator in the Fock space is Gaussian. Examples of Gaussian functions are well-known p.d.f. of Normal distribution, Wigner function, etc. Here, we started with the Normal distribution as an input distribution of continuous-variable (CV) quantum information processing. In our model, the input quantum signal X is in a Gaussian state, and it can be characterized by Gaussian distribution with parameters μ_X and σ_X,

$$X \sim \mathcal{N}(\mu_X, \sigma_X^2)$$

where μ_X and σ_X^2 are the mean and variance of the distribution respectively.

The probability density function (p.d.f.) f_X of X can be expressed as,

$$f_X(x) = \frac{1}{\sigma_X \sqrt{2\pi}} e^{-\frac{1}{2}\left(\frac{x-\mu_X}{\sigma_X}\right)^2} \qquad (8)$$

where μ_X and σ_X are the mean and standard deviation (s.d.) of the distribution. The quantum received signal can be calculated as the convolution product of the Gaussian distributed transmitted signal and the quantum noise signal. As discussed above, important experiments of quantum information processing are done with quantum light.

B. QUANTUM RECEIVED SIGNAL MODEL

The distribution of the transmitted signal X and the hybrid quantum-classical noise Z are independent of each other,

their respective r.v.s are also independent. The input quantum signal is considered in a Gaussian state and follows the Gaussian distribution with p.d.f. f_X, it is continuous, as it is a probability density function. For considering CV signal processing, it modified discrete p.m.f. f_{Z_1} of Poisson quantum noise to a continuous distribution and plugged it with p.d.f. f_{Z_2} of classical Gaussian noise, which is also continuous; hence, the final convolution product f_Z is a continuous function. So both f_X and f_Z are continuous, and X and Z are independent of each other, having relation $Y = X + Z$. Therefore, the p.d.f. f_Y of Y can be written as the convolution of f_X and f_Z as follows:

$$f_Y(y) := \int_{-\infty}^{\infty} f_X(x) f_Z(y-x)\, dx \qquad (9)$$

where Domain of X is given by $\mathcal{D}_X = (-\infty, \infty)$. Consider a range for qubits along a single direction on the surface of the Bloch sphere, such as $\mathcal{D}_X = [0, 2\pi]$ in some restriction. It is discussed in the appendix in detail. This is the same as the range $\mathcal{D}_X = [-\pi, \pi]$, which also represents a single complete rotation on the surface of the sphere. However, this study extends this idea by considering this range as multiple rotations along the great circle; pictorially, it looks like a spiral or a Helix structure. For the theoretical range of the qubit on the Bloch sphere along a circular direction, we can use $\mathcal{D}_X = [-\pi, \pi]$ to represent a single rotation or $\mathcal{D}_X = (-\infty, \infty)$ for multiple rotations ($[-\pi, \pi] \times$ number of rotation).

From using the expressions of (7) and (8) in (9), we have

$$
\begin{aligned}
f_Y(y) &= \int_{-\infty}^{\infty} f_X(x) f_Z(y-x)\, dx \\
&= \int_{-\infty}^{\infty} \left(\frac{1}{\sigma_X \sqrt{2\pi}} e^{-\frac{1}{2}\left(\frac{x-\mu_X}{\sigma_X}\right)^2}\right) \\
&\quad \times \left(\sum_{k=0}^{\infty} \frac{e^{-\lambda}\lambda^k}{k!} \frac{1}{\sigma_{Z_2}\sqrt{2\pi}} e^{-\frac{1}{2}\left(\frac{y-x-k-\mu_{Z_2}}{\sigma_{Z_2}}\right)^2}\right) dx \\
&= \int_{-\infty}^{\infty} \sum_{k=0}^{\infty} \frac{e^{-\lambda}\lambda^k}{k!} \left(\frac{1}{\sigma_X \sqrt{2\pi}} e^{-\frac{1}{2}\left(\frac{x-\mu_X}{\sigma_X}\right)^2}\right) \\
&\quad \times \left(\frac{1}{\sigma_{Z_2}\sqrt{2\pi}} e^{-\frac{1}{2}\left(\frac{y-x-k-\mu_{Z_2}}{\sigma_{Z_2}}\right)^2}\right) dx \qquad (10)
\end{aligned}
$$

Let

$$f(x) := \frac{1}{\sigma_X \sqrt{2\pi}} e^{-\frac{1}{2}\left(\frac{x-\mu_X}{\sigma_X}\right)^2} \qquad (11)$$

and

$$
\begin{aligned}
g(x) &= \frac{1}{\sigma_{Z_2}\sqrt{2\pi}} e^{-\frac{1}{2}\left(\frac{y-x-k-\mu_{Z_2}}{\sigma_{Z_2}}\right)^2} \\
&= \frac{1}{\sigma_{Z_2}\sqrt{2\pi}} e^{-\frac{1}{2}\left(\frac{x-(y-k-\mu_{Z_2})}{\sigma_{Z_2}}\right)^2} \qquad (12)
\end{aligned}
$$

Define $\mu_f := \mu_X$, $\sigma_f := \sigma_X$, $\mu_g := y - k - \mu_{Z_2}$, and $\sigma_g := \sigma_{Z_2}$.

From (11) and (12) we can write

$$f(x) := \frac{1}{\sigma_f \sqrt{2\pi}} e^{-\frac{1}{2}\left(\frac{x-\mu_f}{\sigma_f}\right)^2} \tag{13}$$

and

$$g(x) := \frac{1}{\sigma_g \sqrt{2\pi}} e^{-\frac{1}{2}\left(\frac{x-\mu_g}{\sigma_g}\right)^2} \tag{14}$$

From (13) and (14) the product of functions f and g can be written as

$$f(x)g(x) = \frac{1}{2\pi \sigma_f \sigma_g} e^{-\left[\frac{(x-\mu_f)^2}{2\sigma_f^2} + \frac{(x-\mu_g)^2}{2\sigma_g^2}\right]} \tag{15}$$

Examine the term in the exponent in (15)

$$\beta := \frac{(x-\mu_f)^2}{2\sigma_f^2} + \frac{(x-\mu_g)^2}{2\sigma_g^2}$$

Expanding the terms in quadratics and collecting the terms in the power of x gives,

$$\beta := \frac{(\sigma_f^2 + \sigma_g^2)x^2 - 2(\mu_f \sigma_g^2 + \mu_g \sigma_f^2)x + \mu_f^2 \sigma_g^2 + \mu_g^2 \sigma_f^2}{2\sigma_f^2 \sigma_g^2}$$

Dividing through the coefficient of x^2,

$$\beta := \frac{x^2 - 2\frac{\mu_f \sigma_g^2 + \mu_g \sigma_f^2}{\sigma_f^2 + \sigma_g^2}x + \frac{\mu_f^2 \sigma_g^2 + \mu_g^2 \sigma_f^2}{\sigma_f^2 + \sigma_g^2}}{\frac{2\sigma_f^2 \sigma_g^2}{\sigma_f^2 + \sigma_g^2}}$$

This is again quadratic in x; therefore, (15) is a Gaussian function.

Let us consider,

$$\epsilon = \frac{\left(\frac{\mu_f \sigma_g^2 + \mu_g \sigma_f^2}{\sigma_f^2 + \sigma_g^2}\right)^2 - \left(\frac{\mu_f \sigma_g^2 + \mu_g \sigma_f^2}{\sigma_f^2 + \sigma_g^2}\right)^2}{\frac{2\sigma_f^2 \sigma_g^2}{\sigma_f^2 + \sigma_g^2}} = 0$$

Adding this term to β gives,

$$\beta = \frac{x^2 - 2x\frac{\mu_f \sigma_g^2 + \mu_g \sigma_f^2}{\sigma_f^2 + \sigma_g^2} + \left(\frac{\mu_f \sigma_g^2 + \mu_g \sigma_f^2}{\sigma_f^2 + \sigma_g^2}\right)^2}{\frac{2\sigma_f^2 \sigma_g^2}{\sigma_f^2 + \sigma_g^2}}$$

$$+ \frac{\left(\frac{\mu_f^2 \sigma_g^2 + \mu_g^2 \sigma_f^2}{\sigma_f^2 + \sigma_g^2}\right) - \left(\frac{\mu_f \sigma_g^2 + \mu_g \sigma_f^2}{\sigma_f^2 + \sigma_g^2}\right)^2}{\frac{2\sigma_f^2 \sigma_g^2}{\sigma_f^2 + \sigma_g^2}}$$

$$= \frac{\left(x - \frac{\mu_f \sigma_g^2 + \mu_g \sigma_f^2}{\sigma_f^2 + \sigma_g^2}\right)^2}{\frac{2\sigma_f^2 \sigma_g^2}{\sigma_f^2 + \sigma_g^2}} + \frac{(\mu_f - \mu_g)^2}{2(\sigma_f^2 + \sigma_g^2)}$$

$$= \frac{(x - \mu_{fg})^2}{2\sigma_{fg}^2} + \frac{(\mu_f - \mu_g)^2}{2(\sigma_f^2 + \sigma_g^2)} \tag{16}$$

where

$$\mu_{fg} = \frac{\mu_f \sigma_g^2 + \mu_g \sigma_f^2}{\sigma_f^2 + \sigma_g^2}, \sigma_{fg} = \sqrt{\frac{\sigma_f^2 \sigma_g^2}{\sigma_f^2 + \sigma_g^2}}$$

Substituting (16) in (15) we get,

$$f(x)g(x) = \frac{1}{2\pi \sigma_f \sigma_g} \exp\left[-\frac{(x-\mu_{fg})^2}{2\sigma_{fg}^2}\right] \exp\left[-\frac{(\mu_f - \mu_g)^2}{2(\sigma_f^2 + \sigma_g^2)}\right]$$

Multiplying by $\frac{\sigma_{fg}}{\sigma_{fg}}$ and rearranging gives,

$$f(x)g(x) = \frac{1}{\sqrt{2\pi}\sigma_{fg}} \exp\left[-\frac{(x-\mu_{fg})^2}{2\sigma_{fg}^2}\right]$$

$$\cdot \frac{1}{\sqrt{2\pi(\sigma_f^2 + \sigma_g^2)}} \exp\left[-\frac{(\mu_f - \mu_g)^2}{2(\sigma_f^2 + \sigma_g^2)}\right] \tag{17}$$

Finally from (15) we have,

$$f(x)g(x) = \frac{S_{fg}}{\sqrt{2\pi}\sigma_{fg}} \exp\left[-\frac{(x-\mu_{fg})^2}{2\sigma_{fg}^2}\right] \tag{18}$$

where

$$S_{fg} = \frac{1}{\sqrt{2\pi(\sigma_f^2 + \sigma_g^2)}} \exp\left[-\frac{(\mu_f - \mu_g)^2}{2(\sigma_f^2 + \sigma_g^2)}\right],$$

$$\mu_{fg} = \frac{\mu_f \sigma_g^2 + \mu_g \sigma_f^2}{\sigma_f^2 + \sigma_g^2}, \quad \sigma_{fg} = \sqrt{\frac{\sigma_f^2 \sigma_g^2}{\sigma_f^2 + \sigma_g^2}}$$

and the scaling factor S_{fg} is itself a Gaussian function on both μ_f and μ_g with Gaussian RMS width $\sqrt{(\sigma_f^2 + \sigma_g^2)}$.

Note that the product fg is a Gaussian function. However, μ_{fg} and σ_{fg} need not be mean and s.d. of the distribution fg. The $\mu_f (:= \mu_X)$, $\sigma_f (:= \sigma_X)$ and $\sigma_g (:= \sigma_{Z_2})$ are free from y while only $\mu_g (:= y - k - \mu_{Z_2})$ depends on y. In the integrand below, it is necessary to be careful that both S_{fg} and μ_{fg} contain y and k.

Using these expressions (13), (14), and (15) in (7) gives this result:

$$f_Y(y)$$

$$= \int_{-\infty}^{\infty} \sum_{k=0}^{\infty} \frac{e^{-\lambda}\lambda^k}{k!} \left(\frac{1}{\sigma_f \sqrt{2\pi}} e^{-\frac{1}{2}\left(\frac{x-\mu_f}{\sigma_f}\right)^2}\right)$$

$$\times \left(\frac{1}{\sigma_g \sqrt{2\pi}} e^{-\frac{1}{2}\left(\frac{x-\mu_g}{\sigma_g}\right)^2}\right) dx$$

$$= \int_{-\infty}^{\infty} \sum_{k=0}^{\infty} \frac{e^{-\lambda}\lambda^k}{k!} \frac{S_{fg}}{\sigma_{fg}\sqrt{2\pi}} \exp\left[-\frac{(x-\mu_{fg})^2}{2\sigma_{fg}^2}\right] dx \tag{19}$$

$$= \int_{-\infty}^{\infty} \sum_{k=0}^{\infty} \frac{e^{-\lambda}\lambda^k}{k!} \frac{1}{\sigma_{fg}\sqrt{2\pi}} S_{fg}$$

$$\times \exp\left[-\frac{1}{2\sigma_{fg}^2}\left(x - \frac{\mu_f \sigma_g^2 + \mu_g \sigma_f^2}{\sigma_f^2 + \sigma_g^2}\right)^2\right] dx$$

$$= \int_{-\infty}^{\infty} \sum_{k=0}^{\infty} \frac{e^{-\lambda}\lambda^k}{k!} \frac{1}{\sigma_{fg}\sqrt{2\pi}}$$

$$\cdot \frac{1}{\sqrt{2\pi(\sigma_f^2 + \sigma_g^2)}} \exp\left[-\frac{(\mu_f - \mu_g)^2}{2(\sigma_f^2 + \sigma_g^2)}\right]$$

$$\times \exp\left[-\frac{1}{2\sigma_{fg}^2}\left(x - \frac{\mu_f \sigma_g^2 + (y - k - \mu_{Z_2})\sigma_f^2}{\sigma_f^2 + \sigma_g^2}\right)^2\right] dx$$

$$= \int_{-\infty}^{\infty} \sum_{k=0}^{\infty} \frac{e^{-\lambda}\lambda^k}{k!} \frac{1}{\sigma_{fg}\sqrt{2\pi}}$$

$$\cdot \frac{1}{\sqrt{2\pi(\sigma_f^2 + \sigma_g^2)}} \exp\left[-\frac{(\mu_f - (y - k - \mu_{Z_2}))^2}{2(\sigma_f^2 + \sigma_g^2)}\right]$$

$$\times \exp\left[-\frac{1}{2\sigma_{fg}^2}\left(x - \frac{\mu_f \sigma_g^2 + (y - k - \mu_{Z_2})\sigma_f^2}{\sigma_f^2 + \sigma_g^2}\right)^2\right] dx$$

$$\tag{20}$$

Our target is to interchange the $\sum$ and $\int$.
From (19) consider,

$$f_k(x) := \frac{e^{-\lambda}\lambda^k}{k!} \frac{S_{fg}}{\sigma_{fg}\sqrt{2\pi}} \exp\left[-\frac{(x - \mu_{fg})^2}{2\sigma_{fg}^2}\right]$$

Therefore, we have,

$$f_Y(y) = \int_{-\infty}^{\infty} \sum_{k=0}^{\infty} f_k(x) \, dx$$

This is a special case of Fubini/Tonelli's theorem, where the measures are countable measures on $\mathbb{N}$ and the Lebesgue measure on $\mathbb{R}$ (or, $[0, \infty)$). In particular case:

$$\int_{-\infty}^{\infty} \sum_{k=0}^{\infty} f_k(x) \, dx$$

with $f_k(x)$ being continuous functions $\forall k \in \{0, 1, 2, \ldots\}$.

In deriving the expression for f_Y, it will be easier if one can interchange the integral and the summation in the above case. Another fundamental question will be to find if any necessary and sufficient condition will allow swiping the integral and summation for the above expression.

In particular, Tonelli's theorem says if $f_k(x) \geq 0 \ \forall k, x$ then

$$\int \sum f_k(x) \, dx = \sum \int f_k(x) \, dx \tag{21}$$

without any further conditions needed. The monotone convergence theorem can prove this. Fubini's theorem says that for *a* general function $f_k(\cdot)$, if $\int \sum |f_k(x)| < \infty$ or $\sum \int |f_k(x)| < \infty$ (by Tonelli the two conditions are equivalent), then

$$\int \sum f_k(x) = \sum \int f_k(x)$$

The dominated convergence theorem can prove this. We want to use the condition of Tonelli's theorem in (21). Hence,

we only need to check if $f_k(x) \geq 0 \ \forall k, x$ We have

$$f_k(x) = \frac{e^{-\lambda}\lambda^k}{k!} \frac{S_{fg}}{\sigma_{fg}\sqrt{2\pi}} \exp\left[-\frac{(x - \mu_{fg})^2}{2\sigma_{fg}^2}\right]$$

Since the exponential function is always positive:

$$\therefore \quad \exp\left[-\frac{(x - \mu_{fg})^2}{2\sigma_{fg}^2}\right] \geq 0 \quad \forall x, k$$

For the part

$$\sigma_{fg} = \sqrt{\frac{\sigma_f^2 \sigma_g^2}{\sigma_f^2 + \sigma_g^2}},$$

$\sigma_f(:= \sigma_X)$ and $\sigma_g(:= \sigma_{N_2})$ are standard deviation of distributions X and N_2 respectively and

$$\therefore \sigma_f \geq 0 \quad and \quad \sigma_g \geq 0 \implies \sigma_{fg} \geq 0$$

Similarly, for the part

$$S_{fg} = \frac{1}{\sqrt{2\pi(\sigma_f^2 + \sigma_g^2)}} \exp\left[-\frac{(\mu_f - \mu_g)^2}{2(\sigma_f^2 + \sigma_g^2)}\right],$$

the expression

$$\frac{1}{\sqrt{2\pi(\sigma_f^2 + \sigma_g^2)}} \geq 0$$

as $\sigma_f \geq 0$ and $\sigma_g \geq 0$ and the part

$$\exp\left[-\frac{(\mu_f - \mu_g)^2}{2(\sigma_f^2 + \sigma_g^2)}\right] \geq 0$$

Being exponential function. $\therefore S_{fg} \geq 0$
Let define

$$A := \frac{e^{-\lambda}\lambda^k}{k!}, \quad B := \frac{S_{fg}}{\sqrt{2\pi}\sigma_{fg}}, \quad C := \exp\left[-\frac{(\mu_f - \mu_g)^2}{2(\sigma_f^2 + \sigma_g^2)}\right]$$

$$\tag{22}$$

Note that A and B do not contain x while only C contains x. Since $\lambda \geq 0$, $k \in \{0, 1, 2, \ldots\}$,

$$\therefore A = \frac{e^{-\lambda}\lambda^k}{k!} \geq 0 \quad \forall k, \quad B = \frac{S_{fg}}{\sqrt{2\pi}\sigma_{fg}} \geq 0 \quad \forall k,$$

$$C = \exp\left[-\frac{(\mu_f - \mu_g)^2}{2(\sigma_f^2 + \sigma_g^2)}\right] \geq 0 \quad \forall x, k$$

$$\therefore f_k(x) = A \cdot B \cdot C \geq 0 \quad \forall x, k$$

Hence, from Tonelli's theorem in (21), it can be concluded that the interchanging of $\sum$ and $\int$ in (19) is possible. Hence, from (19), we can write,

$$f_Y(y) = \sum_{k=0}^{\infty} \frac{e^{-\lambda}\lambda^k}{k!} \frac{S_{fg}}{\sigma_{fg}\sqrt{2\pi}} \int_{-\infty}^{\infty} \exp\left[-\frac{(x - \mu_{fg})^2}{2\sigma_{fg}^2}\right] dx$$

$$\tag{23}$$

Remember both S_{fg} and μ_{fg} contain y and k. Now, for the part

$$\int_{-\infty}^{\infty} \exp\left[-\frac{(x-\mu_{fg})^2}{2\sigma_{fg}^2}\right] dx$$

$$= \int_{-\infty}^{\infty} e^{-\left(\frac{x-\mu_{fg}}{\sqrt{2}\sigma_{fg}}\right)^2} dx$$

$$= \int_{-\infty}^{\infty} e^{-t^2} \sqrt{2}\sigma_{fg}\, dt = \sqrt{2}\sigma_{fg} \int_{-\infty}^{\infty} e^{-t^2}\, dt$$

$$= \sqrt{2}\sigma_{fg}\sqrt{\pi} = \sqrt{2\pi}\sigma_{fg} \tag{24}$$

where $t = \frac{x-\mu_{fg}}{\sqrt{2}\sigma_{fg}}$, $\sqrt{2}\sigma_{fg}t + \mu_{fg} = x$, $\sqrt{2}\sigma_{fg}dt = dx$ and $\int_{-\infty}^{\infty} e^{-t^2}\, dt = \sqrt{\pi}$.

Finally, putting expression (24) in (23) we get,

$$f_Y(y) = \sum_{k=0}^{\infty} \frac{e^{-\lambda}\lambda^k}{k!} \frac{S_{fg}}{\sigma_{fg}\sqrt{2\pi}} \sqrt{2\pi}\sigma_{fg}$$

$$= \sum_{k=0}^{\infty} \frac{e^{-\lambda}\lambda^k}{k!} S_{fg}$$

$$= \sum_{k=0}^{\infty} \frac{e^{-\lambda}\lambda^k}{k!} \frac{1}{\sqrt{2\pi(\sigma_f^2 + \sigma_g^2)}} e^{-\frac{1}{2(\sigma_f^2 + \sigma_g^2)}(\mu_f - \mu_g)^2}$$

$$= \sum_{k=0}^{\infty} \frac{e^{-\lambda}\lambda^k}{k!} \frac{1}{\sqrt{2\pi(\sigma_X^2 + \sigma_{Z_2}^2)}} e^{-\frac{(\mu_X - y + k + \mu_{Z_2})^2}{2(\sigma_X^2 + \sigma_{Z_2}^2)}}$$

$$= \sum_{k=0}^{\infty} \frac{e^{-\lambda}\lambda^k}{k!} \frac{1}{\sqrt{2\pi(\sigma_X^2 + \sigma_{Z_2}^2)}} e^{-\frac{(y - k - \mu_X - \mu_{Z_2})^2}{2(\sigma_X^2 + \sigma_{Z_2}^2)}} \tag{25}$$

In order to compare the p.d.f. of noise Z and p.d.f. of received signal Y

$$f_Z(z) = \sum_{k=0}^{\infty} \frac{e^{-\lambda}\lambda^k}{k!} \frac{1}{\sigma_{Z_2}\sqrt{2\pi}} e^{-\frac{(z - k - \mu_{Z_2})^2}{2\sigma_{Z_2}^2}}$$

and

$$f_Y(y) = \sum_{k=0}^{\infty} \frac{e^{-\lambda}\lambda^k}{k!} \frac{1}{\sqrt{2\pi(\sigma_X^2 + \sigma_{Z_2}^2)}} e^{-\frac{(y - k - \mu_X - \mu_{Z_2})^2}{2(\sigma_X^2 + \sigma_{Z_2}^2)}}$$

It is worth noting that mathematically, both p.d.f.s have similar types of expression; moreover, one is a scaled version of the other.

Finally, the differential entropy of the received signal Y is defined by

$$h(Y) = -\int_{\chi_Y} f_Y(y) \log f_Y(y)\, dy$$

where χ_Y is the support of f_Y.

The following section shows the analytical derivations of the differential entropies for quantum noise and received signals. This leads to a closed-form solution of the mutual information and, hence, an analytical expression of capacity. Meanwhile, the upper and lower bounds of the entropies of

the received signal and joint quantum noise have been derived by focusing the Gaussian mixtures model for the noise and the received signal.

VI. GAUSSIAN MIXTURE MODEL

Gaussian mixture models (GMMs) are weighted sums of Gaussian components that approximate arbitrary probability densities [76]. GMM parameters are estimated from data using Expectation-Maximization or maximum a posteriori [77]. GMMs model non-Gaussian uncertainties better than single Gaussians. With enough components, they can approximate any distribution [78]. Differential entropy of GMMs lacks closed form, so bounds are proposed. A novel approximation calculates entropy bounds represented by Gaussian components [79]. Overall, GMMs flexibly model complex multivariate densities using Gaussian components.

A Gaussian mixture model (GMM) is a weighted sum of M component Gaussian densities as given by the equation,

$$f(\mathbf{x}) = \sum_{i=1}^{L} w_i \mathcal{N}(\mathbf{x}, \mu_{\mathbf{i}}, \mathbf{C_i})$$

where w_i are non-negative weighting coefficients with $\sum_i w_i = 1$ and $\mathcal{N}(\mathbf{x}, \mu, \mathbf{C})$ is a Gaussian density mean vector μ, and covariance matrix $\mathbf{C}$.

For a continuous-valued random vector $\bar{x} \in \mathcal{R}^N$ with p.d.f. $f(\bar{x})$, the differential entropy is defined as

$$H(\bar{x}) = E\left[-\log f(\bar{x})\right] = -\int_{\mathcal{R}^N} f(\bar{x})\log f(\bar{x})d\bar{x} \tag{26}$$

The entropy of Gaussian mixtures can not be calculated in the closed form due to the logarithm of a sum of exponential functions. It can be visualized from the expression below

$$H_Z = -\int \sum_i w_i \frac{1}{\sigma\sqrt{2\pi}} e^{-\frac{1}{2}(x-\mu)^T C(x-\mu)}$$
$$\times \left(\log_2 \sum_i w_i \frac{1}{\sigma\sqrt{2\pi}} e^{-\frac{1}{2}(x-\mu)^T C(x-\mu)}\right) dz \tag{27}$$

The exceptional case: For the special case of a single density, where entropy is

$$H(\bar{x}) = \frac{1}{2}\log_2\left((2\pi e)^N \left|\sum\right|\right) \tag{28}$$

an approximate solution of (26). The expression (28) is an upper bound for all Gaussian mixture random vectors with some covariance matrix $\sum$ as in (28).

Independent of the entropy approximation method used, it is generally tricky or even impossible to quantify the deviation between the actual entropy value and its approximation. Providing a close lower and upper bound of the entropy value of a Gaussian mixture random vector makes it possible to decide whether the approximation is meaningful. Furthermore, as we will show, both bounds can be calculated in closed form. Thus, the bounds themselves can be used to efficiently approximate the true entropy value [76].

Theorem 1: A lower bound $H_L(\bar{x})$ of (26) is given by

$$H_L(\bar{x}) = -\sum_{i=0}^{L} w_i \log_2 \left(\sum_{j=0}^{L} w_j m_{i,j} \right) \qquad (29)$$

with $m_{i,j} = \mathcal{N}\left(\bar{\mu}i; \bar{\mu}_j, C_i + C_j \right)$ where μ_i is the mean vector and C_i is the covariance matrix of the corresponding component of Gaussian mixture $f(\bar{x})$.

Theorem 2: An upper bound $H_U(\bar{x})$ of (26) is given by

$$H_U(\bar{x}) = \sum_{i=0}^{L} w_i \log_2 \left(-\log_2 w_i + \frac{1}{2} \log_2 \left((2\pi e)^N \left| C_i \right| \right) \right) \qquad (30)$$

A. IDENTIFYING NOISE MODEL AS GMM
Consider the p.d.f. of joint noise Z in (7),

$$f_Z(z) = \sum_{i=0}^{\infty} \frac{e^{-\lambda} \lambda^i}{i!} \frac{1}{\sigma_{Z_2} \sqrt{2\pi}} e^{-\frac{1}{2} \left(\frac{z-i-\mu_{Z_2}}{\sigma_{Z_2}} \right)^2}$$
$$= \sum_{i=0}^{\infty} u_i \mathcal{N}\left(z, \mu_i^{(z)}, \sigma_i^{(z)2} \right) \qquad (31)$$

where $u_i = \frac{e^{-\lambda} \lambda^i}{i!}$, $\sum_{i=0}^{\infty} u_i = 1$, $u_i \geq 0$ $\forall i$ and $\mathcal{N}(z, \mu_i^{(z)}, \sigma_i^{(z)2})$ is Gaussian density in dummy variable z, mean $\mu_i^{(z)} = \mu_{Z_2} + i$, and $\sigma_i^{(z)2} = \sigma_{Z_2}{}^2$ with standard deviation $\sigma_i^{(z)}$ and variance $\sigma_i^{(z)2}$.

In (31), the approximation of $f_Z(z)$ is taken as

$$f_Z(z) = \sum_{i=0}^{R} \frac{e^{-\lambda} \lambda^i}{i!} \frac{1}{\sigma_{Z_2} \sqrt{2\pi}} e^{-\frac{1}{2} \left(\frac{z-i-\mu_{Z_2}}{\sigma_{Z_2}} \right)^2}$$
$$= \sum_{i=0}^{R} u_i \mathcal{N}\left(z, \mu_i^{(z)}, \sigma_i^{(z)2} \right) \qquad (32)$$

Hence, this led to the compact form,

$$f_Z(z) = \sum_{i=0}^{R} u_i \mathcal{N}\left(z, \mu_i^{(z)}, \sigma_i^{(z)2} \right) \qquad (33)$$

This is the Gaussian mixture in scalar variable z, the coefficient $u_i \geq 0$ $\forall i$ and $\sum_{i=0}^{R} u_i \approx 1$ for large R.

Corresponding Gaussian mixture in random vector $\bar{z} \in \mathbb{R}^M$ is

$$f_Z(\bar{z}) = \sum_{i=0}^{R} u_i \mathcal{N}\left(\bar{z}, \mu_i^{(\bar{z})}, \sum_i^{(z)} \right) \qquad (34)$$

where $\bar{z}$ is the random vector in $\mathbb{R}^M$, $\bar{\mu}_i^{(z)}$ is the mean vector, and $\sum_i^{(z)}$ is the covariance matrix of the corresponding Gaussian density $\mathcal{N}$.

B. IDENTIFYING RECEIVED SIGNAL MODEL AS GMM
Consider the p.d.f of the received signal in (25) given by:

$$f_Y(y) = \sum_{i=0}^{\infty} \frac{e^{-\lambda} \lambda^i}{i!} \frac{1}{\sqrt{2\pi(\sigma_X^2 + \sigma_{Z_2}^2)}} e^{-\frac{(y-i-\mu_X-\mu_{Z_2})^2}{2(\sigma_X^2 + \sigma_{Z_2}^2)}}$$
$$= \sum_{i=0}^{\infty} \frac{e^{-\lambda} \lambda^i}{i!} \frac{1}{\sqrt{2\pi(\sigma_X^2 + \sigma_{Z_2}^2)}} e^{-\frac{1}{2} \left(\frac{y-(i+\mu_X+\mu_{Z_2})}{\sqrt{(\sigma_X^2 + \sigma_{Z_2}^2)}} \right)^2}$$
$$= \sum_{i=0}^{\infty} v_i \mathcal{N}\left(y, \mu_i^{(y)}, \sigma_i^{(y)2} \right) \qquad (35)$$

where $v_i = \frac{e^{-\lambda} \lambda^i}{i!}$, $\sum_{i=0}^{\infty} v_i = 1$, $v_i \geq 0$ $\forall i$ and $\mathcal{N}(y, \mu_i^{(y)}, \sigma_i^{(y)2})$ is Gaussian density in dummy variable y, mean $\mu_i^{(y)} = \mu_X + \mu_{Z_2} + i$, and standard deviation $\sigma_i^{(y)} = \sqrt{(\sigma_X^2 + \sigma_{Z_2}^2)}$ with variance $\sigma_i^{(y)2}$

In practical scenarios simulated over MATLAB, the p.d.f. of hybrid noise in (7) has been approximated as $f(z)$ in (32) and has been used to formulate $f(y)$ which is given by

$$f_Y(y) = \sum_{i=0}^{R} \frac{e^{-\lambda} \lambda^i}{i!} \frac{1}{\sqrt{2\pi(\sigma_X^2 + \sigma_{Z_2}^2)}} e^{-\frac{(y-i-\mu_X-\mu_{Z_2})^2}{2(\sigma_X^2 + \sigma_{Z_2}^2)}}$$
$$= \sum_{i=0}^{R} v_i \mathcal{N}\left(y, \mu_i^{(y)}, \sigma_i^{(y)2} \right) \qquad (36)$$

This is a Gaussian mixture in scalar variable y, and $v_i = \frac{e^{-\lambda} \lambda^i}{i!}$, $v_i \geq 0$ $\forall i$, and $\sum_{i=0}^{R} v_i \approx 1$ for large R.

Corresponding Gaussian mixture in random vector $\bar{y} \in \mathbb{R}^M$ is

$$f_Y(\bar{y}) = \sum_{i=0}^{R} v_i \mathcal{N}\left(\bar{y}, \bar{\mu}_i^{(y)}, \sum_i^{(y)} \right) \qquad (37)$$

where $\bar{y}$ is the random vector in $\mathbb{R}^M$, $\bar{\mu}_i^{(y)}$ is the mean vector, and $\sum_i^{(y)}$ is the covariance matrix of the corresponding Gaussian density $\mathcal{N}$.

Since f_Z and f_Y are both Gaussian mixture densities, the closed-form solution of the corresponding entropies H_Z and H_Y of the noise and the received signal can not be calculated due to the logarithm of the sum and exponential function [76]. However, Theorems 1 and 2 provide the lower and the upper bounds for each entropy H_Z and H_Y. Let us call the upper and lower bounds of H_Z by U_Z and L_Z and the upper and lower bounds of H_Y by U_Y and L_Y, respectively.

That is

$$L_Z \leq H_Z \leq U_Z \qquad (38)$$

and

$$L_Y \leq H_Y \leq U_Y \qquad (39)$$

VII. CAPACITY FOR THE GAUSSIAN INPUT QUANTUM CHANNEL

In [80], the mutual information $I(X; Y)$ between transmitted signal X and received signal Y is defined as $I(X; Y) = H_X + H_Y - H(X, Y)$ and applying the chain rule for continuous variables we have, $H(X, Y) = H(Y|X) - H_X$ Therefore, $I(X; Y) = H_Y - H(Y|X) = H_Y - H(X + Z|X) = H_Y - H(Z|X) = H_Y - H(Z) = H_Y - H_Z$ as transmitted signal X and noise Z are independent. We rename $H(Z)$ as H_Z for notational easiness. Using (38) we will get,

$$-L_Z \geq -H_Z \geq -U_Z$$
$$H_Y - L_Z \geq H_Y - H_Z \geq H_Y - U_Z$$
$$U_Y - L_Z \geq H_Y - L_Z \geq H_Y - H_Z = I(X; Y)$$

Therefore,

$$I(X; Y) \leq U_Y - L_Z \tag{40}$$

Hence,

$$C = \max_{f(x)} I(X; Y) \leq U_Y - L_Z \tag{41}$$

From Theorem 1, let us calculate L_Z, the lower bound for H_Z, as follows:

$$L_Z = -\sum_{i=0}^{R} u_i \log_2 \left(\sum_{j=0}^{R} u_j \mathcal{N}\left(\bar{\mu}_i^{(z)}; \bar{\mu}_j^{(z)}, \sum_i^{(z)} + \sum_j^{(z)} \right) \right) \tag{42}$$

From Theorem 2, similarly we calculate U_Y, the upper bound for H_Y, as follows:

$$U_Y = \sum_{i=0}^{R} v_i \log_2 \left(-\log_2 v_i + \frac{1}{2} \log_2 \left((2\pi e)^M \left| \sum_i^{(y)} \right| \right) \right) \tag{43}$$

where $u_i = v_i = \frac{e^{-\lambda} \lambda^i}{i!} \forall i = 0(1)R$.

From (40), using (42) and (43), we have,

$$U_Y - L_Z$$
$$= \sum_{i=0}^{R} \frac{e^{-\lambda} \lambda^i}{i!} \left(-\log_2 \left(\frac{e^{-\lambda} \lambda^i}{i!} \right) + \frac{1}{2} \log_2 \left((2\pi e)^M \left| \sum_i^{(y)} \right| \right) \right.$$
$$\left. + \log_2 \left(\sum_{j=0}^{R} \frac{e^{-\lambda} \lambda^j}{j!} \mathcal{N}\left(\bar{\mu}_i^{(z)}; \bar{\mu}_j^{(z)}, \sum_i^{(z)} + \sum_j^{(z)} \right) \right) \right) \tag{44}$$

From (41) and (44), the channel capacity would be,

$$C = \sum_{i=0}^{R} \frac{e^{-\lambda} \lambda^i}{i!} \left(-\log_2 \left(\frac{e^{-\lambda} \lambda^i}{i!} \right) \right.$$
$$+ \frac{1}{2} \log_2 \left((2\pi e)^M \left| \sum_i^{(y)} \right| \right)$$
$$\left. + \log_2 \left(\sum_{j=0}^{R} \frac{e^{-\lambda} \lambda^j}{j!} \mathcal{N}\left(\bar{\mu}_i^{(z)}; \bar{\mu}_j^{(z)}, \sum_i^{(z)} + \sum_j^{(z)} \right) \right) \right) \tag{45}$$

This is the expression for the quantum channel capacity when the noise Z and the received signal Y are random vectors of dimension M.

In scalar analogy, that is when the noise Z and the received signal Y are random variables with p.d.f.s (32) and (36) respectively, the expression of capacity reduces to:

$$C = \sum_{i=0}^{R} \frac{e^{-\lambda} \lambda^i}{i!} \left(-\log_2 \left(\frac{e^{-\lambda} \lambda^i}{i!} \right) + \frac{1}{2} \log_2 \left(2\pi.e.\sigma_i^{(y)} \right) \right.$$
$$\left. + \log_2 \left(\sum_{j=0}^{R} \frac{e^{-\lambda} \lambda^j}{j!} \mathcal{N}\left(\mu_i^{(z)}; \mu_j^{(z)}, \sigma_i^{(z)^2} + \sigma_j^{(z)^2} \right) \right) \right) \tag{46}$$

by putting $M = 1$, and replacing $\left| \sum_i^{(y)} \right|$ by $\sigma_i^{(y)}$, $\bar{\mu}_i^{(z)}$ by $\mu_i^{(z)}$, $\bar{\mu}_j^{(z)}$ by $\mu_j^{(z)}$, $\sum_i^{(z)}$ by $\sigma_i^{(z)^2}$ and $\sum_j^{(z)}$ by $\sigma_j^{(z)^2}$, where each vector is replaced by its scalar analogue.

Again $\mu_i^{(z)} = \mu_{Z_2} + i \; \forall i$, $\sigma_i^{(z)^2} = \sigma_{Z_2}^2 \; \forall i$, and $\sigma_i^{(y)^2} = \sigma_X^2 + \sigma_{Z_2}^2 \; \forall i$.

Therefore, the capacity is given by

$$C = \sum_{i=0}^{R} \frac{e^{-\lambda} \lambda^i}{i!} \left(-\log_2 \left(\frac{e^{-\lambda} \lambda^i}{i!} \right) \right.$$
$$+ \frac{1}{2}.\log_2 \left(2\pi.e.\left(\sigma_X^2 + \sigma_{Z_2}^2 \right) \right)$$
$$\left. + \log_2 \left(\sum_{j=0}^{R} \frac{e^{-\lambda} \lambda^j}{j!} \mathcal{N}\left(\mu_{Z_2} + i; \mu_{Z_2} + j, 2\sigma_{Z_2}^2 \right) \right) \right)$$
$$= \sum_{i=0}^{R} \frac{e^{-\lambda} \lambda^i}{i!} \left(-\log_2 \left(\frac{e^{-\lambda} \lambda^i}{i!} \right) \right.$$
$$+ \frac{1}{2}.\log_2 \left(2\pi.e.\left(\sigma_X^2 + \sigma_{Z_2}^2 \right) \right)$$
$$\left. + \log_2 \left(\sum_{j=0}^{R} \frac{e^{-\lambda} \lambda^j}{j!}.\frac{1}{\sqrt{2}\sigma_{Z_2}\sqrt{2\pi}} e^{-\frac{1}{2}\left(\frac{i-j}{\sqrt{2}\sigma_{Z_2}} \right)^2} \right) \right) \tag{47}$$

where

$$\mathcal{N}\left(\mu_{Z_2} + i; \mu_{Z_2} + j, 2\sigma_{Z_2}^2 \right) = \frac{1}{\sqrt{2}\sigma_{Z_2}\sqrt{2\pi}} e^{-\frac{1}{2}\left(\frac{\mu_{Z_2} + i - j - \mu_{Z_2}}{\sqrt{2}\sigma_{Z_2}} \right)^2}.$$

VIII. QUANTUM SIGNAL MODEL FOR NON-GAUSSIAN INPUT

A Gaussian quantum channel does not necessarily imply that the input states are Gaussian [72], [73]. Considering this fact, we consider an arbitrary distribution for the transmitted signal. Hence, the input signal is approximated by its mean and standard deviation $E[X]$ and σ_X, respectively. To invoke the role of the mean and standard deviation of the input state's distribution in the actual scenario, the modified channel equation is considered as follows:

$$Y' = \mu_X + \sigma_X Z \tag{48}$$

where Y' and Z are the channel's received signal and hybrid quantum noise.

Mathematically, the sample space of X can be written as Sp_X and the random variable takes values $X = x_1, x_2, x_2, \ldots$. Since an arbitrary distribution of the transmitted signal X has been considered, we approximate the transmit signal in terms of its point estimate (or mean), μ_X. But to replace the arbitrary input distribution f_X by its mean value is insufficient, as it will not specify the distribution. However, by fixing the mean and standard deviation, one can specify the unknown distribution [81] well. So we replaced the arbitrary input distribution by the mean $E[X]$ and standard deviation σ_X. It is a useful method when considering an unknown distribution for calculations.

However, replacing f_X by $E[X]$ is not meaningful as $E[X]$ ranges from sample space of X, which is $-(\infty, \infty)$, while the mean value of f_X comes from the range of f_X which is $[0, 1]$ as f_X is a p.d.f. A solution to this problem could be replacing the sample space of the input signal by its expected value, that is, $x = E[X] = \mu_X, \forall x \in Sp_X$. This approximation has been made to get a mathematical expression for the output signal and its visualization. Hence, starting with our channel equation

$$Y' = \mu_X + \sigma_X Z$$

and from (7) we have the p.d.f. of the hybrid quantum-classical noise

$$f_Z(z) = \sum_{i=0}^{\infty} \frac{e^{-\lambda}\lambda^i}{i!} \frac{1}{\sigma_{Z_2}\sqrt{2\pi}} e^{-\frac{1}{2}\left(\frac{z-i-\mu_{Z_2}}{\sigma_{Z_2}}\right)^2}$$

Theorem on change of variables: Given the probability density function, $f_Z(z)$, for z, the probability density function (p.d.f.), $f_{Y'}(y')$ for $Y' = aZ + b, (a \neq 0)$, is

$$f_{Y'}(y') = \frac{1}{|a|}f_Z\left(z = \frac{y-b}{a}\right)$$

Putting $a = \mu_X$ and $b = \sigma_X$, we have the received signal model as:

$$
\begin{aligned}
f_{Y'}(y') &= \frac{1}{\sigma_X}f_Z\left(z = \frac{y'-\mu_X}{\sigma_X}\right) \\
&= \frac{1}{\sigma_X}\sum_{i=0}^{\infty}\frac{e^{-\lambda}\lambda^i}{i!}\frac{1}{\sigma_{Z_2}\sqrt{2\pi}}e^{-\frac{1}{2}\left(\frac{\frac{y'-\mu_X}{\sigma_X}-i-\mu_{Z_2}}{\sigma_{Z_2}}\right)^2} \\
&= \sum_{i=0}^{\infty}\frac{e^{-\lambda}\lambda^i}{i!}\frac{1}{\sigma_X\sigma_{Z_2}\sqrt{2\pi}}e^{-\frac{1}{2}\left(\frac{y'-\mu_X-\sigma_X i-\sigma_X \mu_{Z_2}}{\sigma_X \sigma_{Z_2}}\right)^2}
\end{aligned}
$$
(49)

The differential entropy of the received signal Y' is defined by

$$h(Y') = -\int_{\chi_{Y'}} f_{Y'}(y')\log f_{Y'}(y')\,dy'$$

where $\chi_{Y'}$ is the support of $f_{Y'}$.

IX. IDENTIFYING QUANTUM SIGNAL MODELS AS GMMS FOR NON-GAUSSIAN INPUT

Consider the p.d.f of the received signal in (49) given by

$$
\begin{aligned}
f_{Y'}(y') &= \sum_{i=0}^{\infty}\frac{e^{-\lambda}\lambda^i}{i!}\cdot\frac{1}{\sqrt{2\pi}\sigma_X.\sigma_{Z_2}}e^{-\frac{1}{2}\left(\frac{y'-\mu_X-\sigma_X i-\sigma_X \mu_{Z_2}}{\sigma_X.\sigma_{Z_2}}\right)^2} \\
&= \sum_{i=0}^{\infty}v_i.\mathcal{N}\left(y', \mu_i^{(y')}, \sigma_i^{(y')^2}\right)
\end{aligned}
$$
(50)

where $v_i = \frac{e^{-\lambda}\lambda^i}{i!}$, $\sum_{i=0}^{\infty}v_i = 1$, $v_i \geq 0$ $\forall i$ and $\mathcal{N}(y, \mu_i^{(y')}, \sigma_i^{(y')^2})$ is Gaussian density in dummy variable y, mean $\mu_i^{(y)} = \mu_X + \sigma_X i + \sigma_X \mu_{Z_2}$, and standard deviation $\sigma_i^{(y')} = \sigma_X.\sigma_{Z_2}$ with variance $\sigma_i^{(y')^2}$.

In a practical scenario simulated in MATLAB, the p.d.f. of the hybrid noise in (31) can be approximated as $f_Z(z)$ in (32) and can be used to formulate $f_Y(y)$ which is given by

$$
\begin{aligned}
f_{Y'}(y') &= \sum_{i=0}^{R}\frac{e^{-\lambda}\lambda^i}{i!}\cdot\frac{1}{\sqrt{2\pi}\sigma_X.\sigma_{Z_2}}e^{-\frac{1}{2}\left(\frac{y'-\mu_X-\sigma_X i-\sigma_X \mu_{Z_2}}{\sigma_X.\sigma_{Z_2}}\right)^2} \\
&= \sum_{i=0}^{R}v_i.\mathcal{N}\left(y, \mu_i^{(y')}, \sigma_i^{(y')^2}\right)
\end{aligned}
$$
(51)

This is a Gaussian mixture in the scalar variable y', $v_i = \frac{e^{-\lambda}\lambda^i}{i!}$, $v_i \geq 0$ $\forall i$, and $\sum_{i=0}^{\infty}v_i \approx 1$ for large R.

The corresponding Gaussian mixture in a random vector is given by: $\bar{y}' \in \mathbb{R}^M$ is

$$f_Y'(\bar{y}') = \sum_{i=0}^{R}v_i.\mathcal{N}\left(\bar{y}', \bar{\mu}_i^{(y')}, \sum_i^{(y')}\right)$$
(52)

where $\bar{y}'$ is the random vector in $\mathbb{R}^M$, $\bar{\mu}_i^{(y')}$ is the mean vector and $\sum_i^{(y')}$ is the covariance matrix of the corresponding Gaussian density $\mathcal{N}$.

As f_Z and f_Y' are both densities of the Gaussian mixture, the closed-form solution of the corresponding entropies H_Z and H_Y' of noise and the received signal cannot be calculated due to the logarithm of the sum of an exponential function. However, Theorem 1 and 2 provide the lower and upper bound for each of the entropies H_Z and $H_{Y'}$.

The upper bound and lower bound of H_Z are given by U_Z and L_Z in (38) and let the upper and lower bound of $H_{Y'}$ be given by $U_{Y'}$ and $L_{Y'}$, respectively. That is:

$$L_{Y'} \leq H_{Y'} \leq U_{Y'}$$
(53)

X. CAPACITY OF THE QUANTUM CHANNEL FOR NON-GAUSSIAN INPUT

The mutual information $I(X; Y')$ between the transmitted signal X and the received signal Y' is defined as $I(X; Y') = H_X + H_{Y'} - H(X, Y')$ and applying the chain rule for continuous variables we have, $H(X, Y') = H(Y'|X) - H_X$. Therefore, $I(X; Y') = H_{Y'} - H(Y'|X) = H_{Y'} - H(X + Z|X) = H_{Y'} - H(Z|X) = H_{Y'} - H(Z) = H_{Y'} - H_Z$ as transmitted signal X and noise Z are independent. For

the sake of notational easiness, we rename $H(Z)$ as H_Z. Using (53) and (38), we will get,

$$-L_Z \geq -H_Z \geq -U_Z$$
$$H_{Y'} - L_Z \geq H_{Y'} - H_Z \geq H_{Y'} - U_Z$$
$$U_{Y'} - L_Z \geq H_{Y'} - L_Z \geq H_{Y'} - H_Z = I(X; Y')$$

Therefore,

$$I(X; Y') \leq U_{Y'} - L_Z \qquad (54)$$

Hence,

$$\tilde{C} = \max_{f(x)} I(X; Y') \leq U_{Y'} - L_Z \qquad (55)$$

From Theorem 1, as we calculated L_Z, the lower bound for H_Z in (42),

$$L_Z = -\sum_{i=0}^{R} u_i . \log_2 \Big(\sum_{j=0}^{R} u_j . \mathcal{N}\Big(\bar{\mu}_i^{(z)}; \bar{\mu}_j^{(z)}, \sum_i^{(z)} + \sum_j^{(z)}\Big)\Big)$$

From Theorem 2, similarly calculate $U_{Y'}$, the upper bound for $H_{Y'}$,

$$U_{Y'} = \sum_{i=0}^{R} v_i . \log_2 \Big(-\log_2 v_i + \frac{1}{2}.\log_2 \Big((2\pi.e)^M \Big|\sum_i^{(y')}\Big|\Big)\Big) \qquad (56)$$

where $u_i = v_i = \frac{e^{-\lambda}\lambda^i}{i!} \forall i = 0(1)R$. From (42) and (56), we have,

$$U_{Y'} - L_Z$$
$$= \sum_{i=0}^{R} \frac{e^{-\lambda}\lambda^i}{i!}\Big(-\log_2 \Big(\frac{e^{-\lambda}\lambda^i}{i!}\Big)$$
$$+ \frac{1}{2}.\log_2 \Big((2\pi.e)^M \Big|\sum_i^{(y')}\Big|\Big)$$
$$+ \log_2 \Big(\sum_{j=0}^{R} \frac{e^{-\lambda}\lambda^j}{j!}.\mathcal{N}\Big(\bar{\mu}_i^{(z)}; \bar{\mu}_j^{(z)}, \sum_i^{(z)} + \sum_j^{(z)}\Big)\Big)\Big) \qquad (57)$$

From (55) and (57), the channel capacity would be,

$$\tilde{C} = \sum_{i=0}^{R} \frac{e^{-\lambda}\lambda^i}{i!}\Big(-\log_2 \Big(\frac{e^{-\lambda}\lambda^i}{i!}\Big)$$
$$+ \frac{1}{2}.\log_2 \Big((2\pi.e)^M \Big|\sum_i^{(y')}\Big|\Big)$$
$$+ \log_2 \Big(\sum_{j=0}^{R} \frac{e^{-\lambda}\lambda^j}{j!}.\mathcal{N}\Big(\bar{\mu}_i^{(z)}; \bar{\mu}_j^{(z)}, \sum_i^{(z)} + \sum_j^{(z)}\Big)\Big)\Big) \qquad (58)$$

This is the expression for the quantum channel capacity when the noise Z and the received signal Y' are random vectors of dimension M.
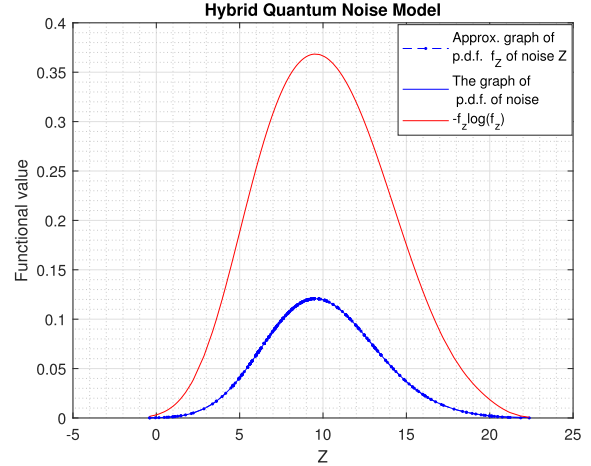
FIGURE 4. Quantum Noise model as a convolution of AWGN and Poissonian quantum noise.

In scalar analogy, that is when the noise Z and the received signal Y' are random variables with p.d.f.s (32) and (51) respectively, the expression of capacity reduces to:

$$\tilde{C} = \sum_{i=0}^{R} \frac{e^{-\lambda}\lambda^i}{i!}\Big(-\log_2 \Big(\frac{e^{-\lambda}\lambda^i}{i!}\Big) + \frac{1}{2}.\log_2 \Big(2\pi.e.\sigma_i^{(y')}\Big)$$
$$+ \log_2 \Big(\sum_{j=0}^{R} \frac{e^{-\lambda}\lambda^j}{j!}.\mathcal{N}\Big(\mu_i^{(z)}; \mu_j^{(z)}, \sigma_i^{(z)^2} + \sigma_j^{(z)^2}\Big)\Big)\Big) \qquad (59)$$

by putting $M = 1$, and replacing $\Big|\sum_i^{(y')}\Big|$ by $\sigma_i^{(y')}$, $\bar{\mu}_i^{(z)}$ by $\mu_i^{(z)}$, $\bar{\mu}_j^{(z)}$ by $\mu_j^{(z)}$, $\sum_i^{(z)}$ by $\sigma_i^{(z)^2}$ and $\sum_j^{(z)}$ by $\sigma_j^{(z)^2}$, where each vector is replaced by its scalar analogue.

Again $\mu_i^{(z)} = \mu_{Z_2} + i \ \forall i$, $\sigma_i^{(z)^2} = \sigma_{Z_2}^2 \ \forall i$, and $\sigma_i^{(y')^2} = \sigma_X^2 \sigma_{Z_2}^2 \ \forall i$.
Therefore, the capacity

$$\tilde{C}$$
$$= \sum_{i=0}^{R} \frac{e^{-\lambda}\lambda^i}{i!}\Big(-\log_2 \Big(\frac{e^{-\lambda}\lambda^i}{i!}\Big) + \frac{1}{2}.\log_2 \Big(2\pi.e.\big(\sigma_X^2 \sigma_{Z_2}^2\big)\Big)$$
$$+ \log_2 \Big(\sum_{j=0}^{R} \frac{e^{-\lambda}\lambda^j}{j!}.\mathcal{N}\Big(\mu_{Z_2} + i; \mu_{Z_2} + j, 2\sigma_{Z_2}^2\Big)\Big)\Big)$$
$$= \sum_{i=0}^{R} \frac{e^{-\lambda}\lambda^i}{i!}\Big(-\log_2 \Big(\frac{e^{-\lambda}\lambda^i}{i!}\Big) + \frac{1}{2}.\log_2 \Big(2\pi.e.\big(\sigma_X^2 \sigma_{Z_2}^2\big)\Big)$$
$$+ \log_2 \Big(\sum_{j=0}^{R} \frac{e^{-\lambda}\lambda^j}{j!}.\frac{1}{\sqrt{2}\sigma_{Z_2}\sqrt{2\pi}}e^{-\frac{1}{2}\left(\frac{i-j}{\sqrt{2}\sigma_{Z_2}}\right)^2}\Big)\Big) \qquad (60)$$

where

$$\mathcal{N}\Big(\mu_{Z_2} + i; \mu_{Z_2} + j, 2\sigma_{Z_2}^2\Big) = \frac{1}{\sqrt{2}\sigma_{Z_2}\sqrt{2\pi}}e^{-\frac{1}{2}\left(\frac{\mu_{Z_2}+i-j-\mu_{Z_2}}{\sqrt{2}\sigma_{Z_2}}\right)^2}.$$
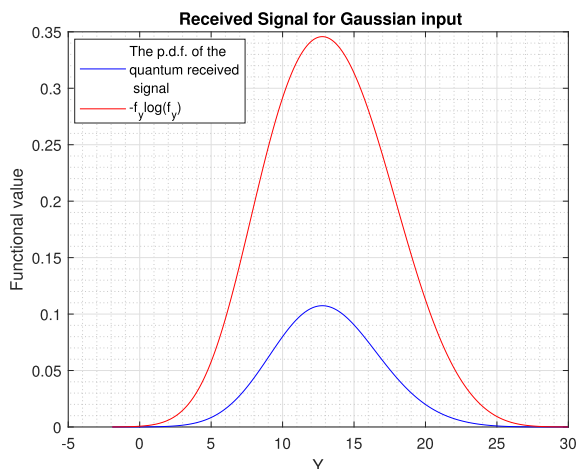
FIGURE 5. Received signal in case of Gaussian input, considered as a convoluted function of the quantum noise field and Gaussian transmitted signal for the Gaussian quantum channel.
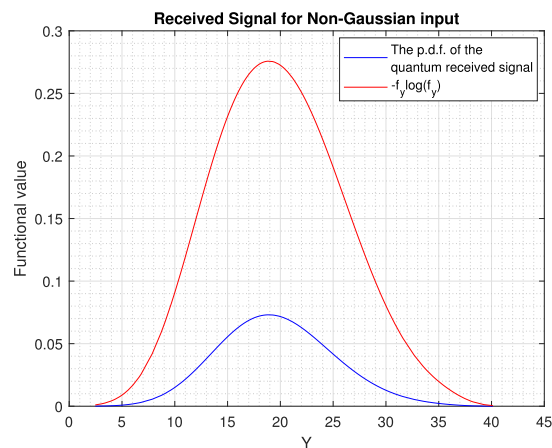
XI. NUMERICAL ANALYSIS

A. NOISE MODEL VISUALISATION

To visualize the models, consider the two following functions:

$$f_Z(z) = \sum_{n=0}^{\infty} \frac{e^{-\lambda}\lambda^n}{n!} \frac{1}{\sigma_{Z_2}\sqrt{2\pi}} e^{-\frac{1}{2}\left(\frac{z-n-\mu_{Z_2}}{\sigma_{Z_2}}\right)^2}$$

and

$$\tilde{f}_Z(z) = \sum_{n=0}^{R} \frac{e^{-\lambda}\lambda^n}{n!} \frac{1}{\sigma_{Z_2}\sqrt{2\pi}} e^{-\frac{1}{2}\left(\frac{z-n-\mu_{Z_2}}{\sigma_{Z_2}}\right)^2}$$

Theoretically, the density function f_Z is the actual p.d.f. of Z and the function $\tilde{f}_Z$ is an approximated p.d.f. of Z shown in Fig. 4. The figure shows the hybrid quantum noise model for parameter $\lambda = 10$, and the sample sizes of the underlying component noises Z_1 and Z_2 are 20 for each distribution (Poisson and Gaussian). Each simulation in MATLAB randomly selects two sample spaces for the Poisson distribution (with parameter $\lambda = 10$) and the Gaussian distribution (with parameters $\mu_{Z_2} = 0$ and $\sigma_{Z_2} = 1$), returning a joint sample space for Z.

Let A and B be two sets, and $f : A \rightarrow B$ and $g : A \rightarrow B$ are two functions. Mathematically, two functions are identical if $f(a) = g(a) \ \forall \ a \in A$. In particular, the domains of the functions f_Z and $\tilde{f}_Z$ are the same as they are the same sample space of Z, and $f_Z(z) = \tilde{f}_Z(z) \ \forall z \in Z$. Therefore the actual p.d.f. f_Z of Z can be well approximated by the function $\tilde{f}_Z$ in Fig. 4. From here onwards, we will refer $\tilde{f}_Z$ by f_Z. Since the noise model is identified as GMM, we can infer that the p.d.f. can be approximated as a mixture of the finite number of Gaussian densities [76]. In Fig. 4, we characterize the joint quantum-classical noise by plotting the function $-f_Z(z) \log_2 f_Z(z)$ and $f_Z(z)$. This will be used to calculate the mutual information $I(X; Y)$, along with the entropy of received signal Y and hence the channel capacity of the quantum channel.

FIGURE 6. Received signal in case of non-Gaussian input, considered as a convoluted function of quantum noise field and non-Gaussian transmitted signal for Gaussian quantum channel.

B. OUTPUT SIGNAL MODEL'S VISUALISATION

1) RECEIVED SIGNAL MODEL'S VISUALISATION FOR GAUSSIAN DISTRIBUTED TRANSMITTED SIGNAL FOR GAUSSIAN QUANTUM CHANNEL

The p.d.f. of the received signal f_Y is given in Fig. 5, which is the convolution product of the p.d.f.-s of the Gaussian transmitted signal and mixed quantum noise. Therefore, we computed the approximate density function for the received signal Y. Since the output signal model is identified as GMM, we can infer that the p.d.f. can be approximated as a mixture of the finite number of Gaussian densities [76]. We also characterized the function $-f_Y(y)log_2 f_Y(y)$ shown in Fig. 5 whose integral is the entropy of the received signal Y.

2) RECEIVED SIGNAL MODEL'S VISUALIZATION FOR A NON-GAUSSIAN DISTRIBUTED TRANSMITTED SIGNAL FOR GAUSSIAN QUANTUM CHANNEL

The p.d.f. of the received signal $f_{Y'}$ is given in Fig. 6, we approximated the probability distribution of the transmitted signal X by the mean of the sample space of X, and based on that we calculated the approximate density function for the received signal Y'. Since the received signal model is identified as GMM, we can infer that the p.d.f. can be approximated as a mixture of the finite number of Gaussian densities [76]. We also characterized the function $-f_{Y'}(y')log_2 f_{Y'}(y')$ shown in fig. 6 whose integral is the entropy of the received signal Y'.

C. CAPACITY COMPARISONS WITH RESPECT TO SIGNAL-TO-NOISE RATIO

1) VISUALISATION OF THE CAPACITY TREND WITH SNR FOR A GAUSSIAN QUANTUM CHANNEL IN CASE OF NON-GAUSSIAN DISTRIBUTED TRANSMITTED SIGNAL

In Fig. 7 the capacity of the noisy quantum channel for the non-Gaussian distributed transmitted signal with respect to signal-to-noise ratio (SNR) and the logarithm of signal-to-noise ratio ($\log_2(SNR)$), are illustrated. The capacity increases with SNR and the logarithm of SNR,
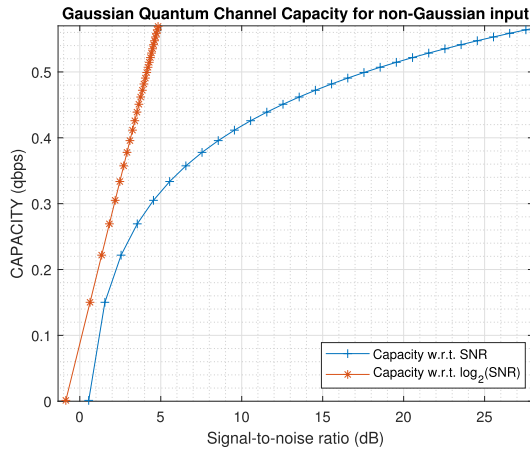
FIGURE 7. The channel capacity of the Gaussian quantum channel for the non-Gaussian input transmitted signal.
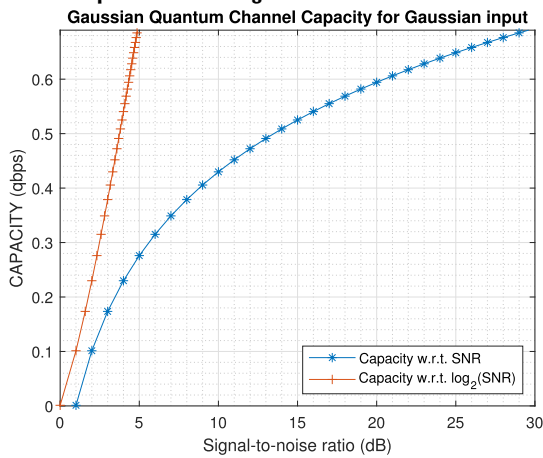

FIGURE 8. The channel capacity of the Gaussian quantum channel for the Gaussian input transmitted signal.

as expected. However, in the next subsection, we will visualize the tendency of the capacity of the Gaussian quantum channel in the case of non-Gaussian input transmitted signal, and these will lead to comparing the capacities for Gaussian and non-Gaussian inputs for the Gaussian quantum channel.

2) VISUALISATION OF THE CAPACITY TREND WITH SNR FOR GAUSSIAN QUANTUM CHANNEL IN CASE OF GAUSSIAN DISTRIBUTED TRANSMITTED SIGNAL

Fig. 8 shows the capacity of the noisy quantum channel as functions of SNR and the logarithm of SNR in the case of Gaussian distributed input. It can be observed that the capacity increases with SNR and and the logarithm of SNR, as expected. However, in the next section, we would like to compare the tendency of the capacities of the Gaussian quantum channels in either case of Gaussian and the non-Gaussian transmitted signal.

3) COMPARISON OF THE CAPACITY TENDENCIES OF GAUSSIAN QUANTUM CHANNEL IN CASE OF GAUSSIAN AND NON-GAUSSIAN DISTRIBUTED TRANSMITTED SIGNAL

The capacity figures, Fig. 7 and Fig. 8 show the capacities of single Gaussian Quantum channels for non-Gaussian and

Gaussian transmitted signals, respectively, with respect to (I) signal to noise ratio and (II) the logarithm of SNR. To conclude, the Gaussian transmitted signal gives better capacity (the highest achievable data transmission rate) for the quantum channel shown in Fig. 8, meanwhile, the non Gaussian transmitted signal for the Gaussian channel gives a bit lesser capacity rate (shown in Fig. 7) than the Gaussian inputted transmitted signal with respect to signal to noise ratio. In compare to the logarithm of SNR as well, Gaussian input signal gives better capacity than the non-Gaussian input for the same channel, for the Gaussian quantum channel, which matches with standard results for capacity with respect to SNR for classical communication.

XII. CONCLUSION

This research advances statistical quantum signal processing by modeling Gaussian quantum channels. It has developed representations for hybrid quantum noise channel models and output signals in these channels. Despite using Gaussian mixture models to characterize the quantum noise statistics, closed-form solutions are derived for the channel capacities with Gaussian and non-Gaussian inputs. The capacity expressions quantitatively demonstrate that Gaussian input distributions yield the highest achievable data rates for Gaussian quantum channels across varying signal-to-noise ratios. This research thus makes several vital contributions: (i) graphical depictions of hybrid quantum noise, (ii) statistical frameworks to describe quantum Gaussian channels, and (iii) analytical capacity solutions that confirm the advantage of Gaussian signaling in this setting. Overall, the modeling and analyzing of quantum Gaussian channels from a statistical signal processing perspective provides new insights into optimizing information transfer through quantum networks.

APPENDIX
APPROXIMATING THE QUBIT BY A SINGLE VARIABLE FUNCTION

- *Assumption related to joint quantum noise effects:* Classical communication theory finds that the bits will remain within a specific region of the actual position [82] due to a specific range of noise power, which is practically observed. Although the bit may travel beyond this region, in that case, the noise power would be extremely high, which is not usually observed in practice. The quantum noise can generally be observed when the classical noise has been suppressed. We are simultaneously considering the classical and quantum noise. Considering the above noise power theory is a straightforward choice, as the classical noise is integrated with the quantum system, and its effects should be reflected in the calculations. In connection with control theory, we can infer that within a specific (practical) range of the joint noise power, the qubit will not move far beyond its actual position due to the joint
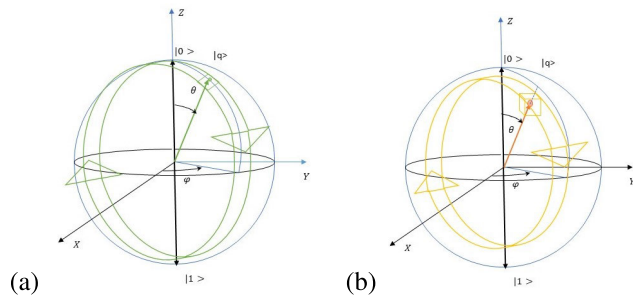
FIGURE 9. (a) Case I: Representation of a pure state qubit on the Bloch sphere, and (b) Case II: Representation of a mixed state qubit inside the Bloch sphere.

noise effect. This works for both the pure state and the mixed state qubits.

- **Representation of a qubit:** Case I: *A pure state qubit can be represented by a point (θ, ϕ) on the Bloch sphere:* A qubit on the Bloch sphere can be viewed as a pure-state qubit. It can be represented by a vector (θ, ϕ) on the surface of the sphere, and it can be represented by a bivariate function $\zeta(\theta, \phi)$, it is clear from the notation that ζ is bivariate function, whose arguments are θ and ϕ, which we call variables x_1 and x_2 respectively. Let us consider the pure-state qubit, and we will discuss how its position is affected by the noise power. Since the pure qubit is lying on the surface of the Bloch sphere, the qubit can be represented as a vector (θ, ϕ) of dimension 2. We assume that within a certain noise power the qubit will remain within a complete strip along the surface of the Bloch sphere. In particular, we consider a circular path along the surface of the sphere, which will be the path of the qubit if the qubit is rotated by varying θ while keeping ϕ constant. Now consider a strip along the surface of the sphere that contains the path circle of the qubit in the middle, then the distance from the qubit on the circle to the edges of the strip will be δ on each side. Hence, the breath of the strip will be 2δ shown in Fig. 9(a). We consider that if the qubit experiences a certain (practically feasible) range of noise power, then the position of the qubit will not end up far beyond the indicated region (the strip). Mathematically, we considered $(\theta, \phi) \mapsto (\tilde{\theta}, \phi \pm \delta)$ where $\tilde{\theta} \in [0, 2\pi]$. To reduce the computational complexity of the problem, we infer that δ will be so small that the second variable ϕ can be considered constant with respect to θ.

Case II: *A mixed qubit can be represented by a point (θ, ϕ, r) inside the Bloch sphere:* A qubit inside the Bloch sphere can be viewed as a mixed-state qubit. It can be represented by a vector (θ, ϕ, r) inside the sphere, and it can be represented by a multivariate function $\tilde{\zeta}(\theta, \phi, r)$, whose arguments are θ, ϕ and r, which we call variables x_1, x_2 and x_3 respectively. Let us consider the mixed state qubit, and we will discuss its position affected by the noise power. When we are dealing with the qubit that lies inside the Bloch sphere, the mixed state qubit can be represented as a

vector (θ, ϕ, r), where r is the distance of the qubit from the center of the sphere. In connection to classical communication theory, we assumed that within a certain (feasible) range of noise power, the qubit would remain within a torus/tunnel-like object (whose cross section is square) inside the Bloch sphere. Consider a circular path inside the sphere, which will be the path of the qubit if one rotates the qubit by varying θ while keeping ϕ and r constant. Now consider a torus/tunnel-like object (whose cross section is square) inside the sphere that contains the path circle of the qubit in the middle; the distance from the qubit on the circle to the sides of the tunnel will be δ on each side of the cube. Therefore, the area of the cross-sectional region (which is a square) will be 2δ x 2δ shown in Fig. 9(b). We consider that if the qubit experiences a certain (practically feasible) range for the noise power, then the position of the qubit will not go far beyond the indicated region (the torus/ tunnel). Mathematically, we considered $(\theta, \phi, r) \mapsto (\tilde{\theta}, \phi \pm \delta_1, r \pm \delta_2)$ where $\tilde{\theta} \in [0, 2\pi]$. To reduce the complexity, we can infer that the cuboid region can be approximated by the cube region discussed above. Hence we have, $(\theta, \phi, r) \mapsto (\tilde{\theta}, \phi \pm \delta, r \pm \delta)$ where $\tilde{\theta} \in [0, 2\pi]$. We expect that δ will be so small that the second and third variables ϕ and r can be considered constant concerning the first variable θ. Therefore, we have $(\theta, \phi, r) \mapsto (\tilde{\theta}, \phi, r)$ where $\tilde{\theta} \in [0, 2\pi]$.

- In summary, this approximation can be done by varying any of the variables θ and ϕ at a time, considering the other variables as constant concerning the said variable. In our case, we varied θ, considering the remaining variables as constant.

REFERENCES

[1] N. Gisin, G. Ribordy, W. Tittel, and H. Zbinden, "Quantum cryptography," *Rev. Mod. Phys.*, vol. 74, no. 1, pp. 145–195, Mar. 2002, doi: 10.1103/RevModPhys.74.145.

[2] L. Gyongyosi and S. Imre, "A survey on quantum computing technology," *Comput. Sci. Rev.*, vol. 31, pp. 51–71, Feb. 2019.

[3] G. Alber, T. Beth, M. Horodecki, P. Horodecki, R. Horodecki, M. Rötteler, H. Weinfurter, R. Werner, and A. Zeilinger, *Quantum Information: An Introduction to Basic Theoretical Concepts and Experiments*, vol. 173. Germany: Springer, 2003.

[4] C. H. Bennett and G. Brassard, "Quantum cryptography: Public key distribution and coin tossing," *Theor. Comput. Sci.*, vol. 560, pp. 7–11, Dec. 2014.

[5] V. Scarani, H. Bechmann-Pasquinucci, N. J. Cerf, M. Dušek, N. Lütkenhaus, and M. Peev, "The security of practical quantum key distribution," *Rev. Mod. Phys.*, vol. 81, pp. 1301–1350, Sep. 2009.

[6] A. K. Ekert, "Quantum cryptography based on Bell's theorem," *Phys. Rev. Lett.*, vol. 67, pp. 661–663, Aug. 1991.

[7] T. Jennewein, C. Simon, G. Weihs, H. Weinfurter, and A. Zeilinger, "Quantum cryptography with entangled photons," *Phys. Rev. Lett.*, vol. 84, no. 20, pp. 4729–4732, May 2000.

[8] H.-J. Briegel, W. Dür, J. I. Cirac, and P. Zoller, "Quantum repeaters: The role of imperfect local operations in quantum communication," *Phys. Rev. Lett.*, vol. 81, no. 26, pp. 5932–5935, Dec. 1998.

[9] S. Pirandola, J. Eisert, C. Weedbrook, A. Furusawa, and S. L. Braunstein, "Advances in quantum teleportation," *Nature Photon.*, vol. 9, no. 10, pp. 641–652, Oct. 2015.

[10] H. J. Kimble, "The quantum internet," *Nature*, vol. 453, no. 7198, pp. 1023–1030, Jun. 2008.

[11] S. Wehner, D. Elkouss, and R. Hanson, "Quantum Internet: A vision for the road ahead," *Science*, vol. 362, no. 6412, Oct. 2018, Art. no. eaam9288.

[12] J. Illiano, M. Caleffi, A. Manzalini, and A. S. Cacciapuoti, "Quantum Internet protocol stack: A comprehensive survey," *Comput. Netw.*, vol. 213, Aug. 2022, Art. no. 109092. [Online]. Available: https://www.sciencedirect.com/science/article/pii/S1389128622002250

[13] S. Santos, F. A. Monteiro, B. C. Coutinho, and Y. Omar, "Shortest path finding in quantum networks with quasi-linear complexity," *IEEE Access*, vol. 11, pp. 7180–7194, Jan. 2023.

[14] J. An, H. Li, D. W. K. Ng, and C. Yuen, "Fundamental detection probability vs. achievable rate tradeoff in integrated sensing and communication systems," *IEEE Trans. Wireless Commun.*, vol. 22, no. 12, pp. 9835–9853, Dec. 2023.

[15] M. A. Nielsen and I. L. Chuang, *Quantum Computation and Quantum Information: 10th Anniversary Edition*. Cambridge, U.K.: Cambridge Univ. Press, 2010.

[16] S. Resch and U. R. Karpuzcu, "Benchmarking quantum computers and the impact of quantum noise," *ACM Comput. Surv.*, vol. 54, no. 7, pp. 1–35, Jul. 2021.

[17] S. Castelletto, I. P. Degiovanni, and M. L. Rastello, "Quantum and classical noise in practical quantum-cryptography systems based on polarization-entangled photons," *Phys. Rev. A, Gen. Phys.*, vol. 67, no. 2, Feb. 2003, Art. no. 022305.

[18] H. Paul, "Photon antibunching," *Rev. Mod. Phys.*, vol. 54, no. 4, pp. 1061–1102, Oct. 1982.

[19] D. Renker and E. Lorenz, "Advances in solid state photon detectors," *J. Instrum.*, vol. 4, pp. 4004–4052, Apr. 2009, doi: 10.1088/1748-0221/4/04/P04004.

[20] E. Eleftheriadou, S. M. Barnett, and J. Jeffers, "Quantum optical state comparison amplifier," *Phys. Rev. Lett.*, vol. 111, no. 21, p. 213601, Nov. 2013, doi: 10.1103/PhysRevLett.111.213601.

[21] F. W. Strauch, "Relativistic quantum walks," *Phys. Rev. A, Gen. Phys.*, vol. 73, no. 5, May 2006, Art. no. 054302.

[22] M. O. Scully and M. S. Zubairy, *Quantum Optics*. Cambridge, U.K.: Cambridge Univ. Press, 1997.

[23] P. H. Handel, "Quantum approach to $1/f$ noise," *Phys. Rev. A, Gen. Phys.*, vol. 22, no. 2, p. 745, Aug. 1980.

[24] V. Koryukin, "Modeling a semiconductor quantum dot laser," in *Proc. Int. Conf. Laser Opt. (LO)*, St. Petersburg, Russia, Jun. 2016, p. R3-35, doi: 10.1109/LO.2016.7549745.

[25] P. Kultavewuti, E. Y. Zhu, L. Qian, V. Pusino, M. Sorel, and J. S. Aitchison, "Correlated photon pair generation in AlGaAs nanowaveguides via spontaneous four-wave mixing," *Opt. Exp.*, vol. 24, no. 4, pp. 3365–3376, Feb. 2016.

[26] J. B. Johnson, "Thermal agitation of electricity in conductors," *Phys. Rev.*, vol. 32, no. 1, pp. 97–109, Jul. 1928.

[27] W. Schottky, "Über spontane Stromschwankungen in verschiedenen Elektrizitätsleitern," *Ann. Phys.*, vol. 362, pp. 541–567, 1918.

[28] D. B. Leeson, "A simple model of feedback oscillator noise spectrum," *Proc. IEEE*, vol. 54, no. 2, pp. 329–330, Feb. 1966.

[29] R. F. Voss, "1/f (flicker) noise: A brief review," in *Proc. 33rd Annu. Symp. Freq. Control*, May 1979, pp. 40–46.

[30] S. Donati, "Photodetectors: Devices, circuits, and applications," *Meas. Sci. Technol.*, vol. 12, no. 5, p. 653, May 2001.

[31] W. Van Roosbroeck, "Theory of the flow of electrons and holes in germanium and other semiconductors," *Bell Syst. Tech. J.*, vol. 29, no. 4, pp. 560–607, Oct. 1950.

[32] F. N. Hooge, "$1/f$ noise is no surface effect," *Phys. Lett. A*, vol. 29, no. 3, pp. 139–140, 1969.

[33] M. J. Buckingham, *Noise in Electronic Devices and Systems* (Electrical and Electronic Engineering Series). New York, NY, USA: E. Horwood, 1983.

[34] H.-T. Lim, J.-C. Lee, K.-H. Hong, and Y.-H. Kim, "Avoiding entanglement sudden death using single-qubit quantum measurement reversal," *Opt. Exp.*, vol. 22, no. 16, pp. 19055–19068, 2014. [Online]. Available: https://api.semanticscholar.org/CorpusID:19420592

[35] K. C. Lee, M. R. Sprague, B. J. Sussman, J. Nunn, N. K. Langford, X.-M. Jin, T. Champion, P. Michelberger, K. F. Reim, D. England, D. Jaksch, and I. A. Walmsley, "Entangling macroscopic diamonds at room temperature," *Science*, vol. 334, no. 6060, pp. 1253–1256, Dec. 2011.

[36] H. Kang, D. Han, N. Wang, Y. Liu, S. Hao, and X. Su, "Experimental demonstration of robustness of Gaussian quantum coherence," *Photon. Res.*, vol. 9, no. 7, pp. 1330–1335, Jul. 2021.

[37] C. Weedbrook, S. Pirandola, R. García-Patrón, N. J. Cerf, T. C. Ralph, J. H. Shapiro, and S. Lloyd, "Gaussian quantum information," *Rev. Mod. Phys.*, vol. 84, p. 621, May 2012.

[38] J. Preskill, "Lecture notes for physics 219: Quantum computation," California Inst. Technol., Pasadena, CA, USA, 1999, vol. 7.

[39] D. Aharonov, A. Kitaev, and J. Preskill, "Fault-tolerant quantum computation with long-range correlated noise," *Phys. Rev. Lett.*, vol. 96, no. 5, p. 2190, Feb. 2006.

[40] D. A. Lidar and K. B. Whaley, "Decoherence-free subspaces and subsystems," in *Irreversible Quantum Dynamics*. Berlin, Germany: Springer, Jun. 2003, pp. 83–120.

[41] C. H. Bennett and S. J. Wiesner, "Communication via one- and two-particle operators on Einstein–Podolsky–Rosen states," *Phys. Rev. Lett.*, vol. 69, no. 20, pp. 2881–2884, Nov. 1992.

[42] D. Gottesman, "Stabilizer codes and quantum error correction," 1997, arXiv:quant-ph/9705052. [Online]. Available: https://api.semanticscholar.org/CorpusID:118824832

[43] J. Preskill. (2000). *Quantum Information and Computation*. [Online]. Available: http://www.theory.caltech.edu/people/preskill/ph229/

[44] P. W. Shor, "Scheme for reducing decoherence in quantum computer memory," *Phys. Rev. A, Gen. Phys.*, vol. 52, no. 4, pp. R2493–R2496, Oct. 1995.

[45] D. Gottesman, "An introduction to quantum error correction and fault-tolerant quantum computation," in *Proc. Symp. Appl. Math.*, vol. 68, 2010, pp. 13–58.

[46] D. Chandra, Z. B. Kaykac Egilmez, Y. Xiong, S. X. Ng, R. G. Maunder, and L. Hanzo, "Universal decoding of quantum stabilizer codes via classical guesswork," *IEEE Access*, vol. 11, pp. 19059–19072, Feb. 2023.

[47] D. Cruz, F. A. Monteiro, and B. C. Coutinho, "Quantum error correction via noise guessing decoding," *IEEE Access*, vol. 11, pp. 119446–119461, Oct. 2023.

[48] Z. Babar, D. Chandra, H. V. Nguyen, P. Botsinis, D. Alanis, S. X. Ng, and L. Hanzo, "Duality of quantum and classical error correction codes: Design principles and examples," *IEEE Commun. Surveys Tuts.*, vol. 21, no. 1, pp. 970–1010, 1st Quart., 2019.

[49] B. Gu and I. Franco, "When can quantum decoherence be mimicked by classical noise?" *J. Chem. Phys.*, vol. 151, no. 1, Jul. 2019.

[50] J. Bergli, Y. M. Galperin, and B. L. Altshuler, "Decoherence in qubits due to low-frequency noise," *New J. Phys.*, vol. 11, no. 2, pp. 1367–2630, Feb. 2009, doi: 10.1088/1367-2630/11/2/025002.

[51] R.-D. Li and P. Kumar, "Quantum-noise reduction in traveling-wave second-harmonic generation," *Phys. Rev. A, Gen. Phys.*, vol. 49, no. 3, pp. 2157–2166, 1994.

[52] H. Cramér, *Mathematical Methods of Statistics*. Princeton, NJ, USA: Princeton Univ. Press, 1946.

[53] C. M. Caves, "Quantum-mechanical noise in an interferometer," *Phys. Rev. D, Part. Fields*, vol. 23, no. 8, pp. 1693–1708, Apr. 1981.

[54] V. Giovannetti and S. Mancini, "Bosonic memory channels," *Phys. Rev. A, Gen. Phys.*, vol. 71, no. 6, Jun. 2005, doi: 10.1103/physreva.71.062304.

[55] K. Jacobs and D. A. Steck, "A straightforward introduction to continuous quantum measurement," *Contemp. Phys.*, vol. 47, no. 5, pp. 279–303, Sep. 2006.

[56] A. Chenu, M. Beau, J. Cao, and A. del Campo, "Quantum simulation of many-body decoherence: Noise as a resource," Aug. 2016.

[57] A. Ishizaki and G. R. Fleming, "Unified treatment of quantum coherent and incoherent hopping dynamics in electronic energy transfer: Reduced hierarchy equation approach," *J. Chem. Phys.*, vol. 130, no. 23, Jun. 2009, Art. no. 234111.

[58] N. Gisin and I. C. Percival, "The quantum-state diffusion model applied to open systems," *J. Phys. A, Math. Gen.*, vol. 25, no. 21, pp. 5677–5691, Nov. 1992.

[59] O.-P. Saira, M. Möttönen, V. F. Maisi, and J. P. Pekola, "Environmentally activated tunneling events in a hybrid single-electron box," *Phys. Rev. B, Condens. Matter*, vol. 82, no. 15, p. 155443, Oct. 2010, doi: 10.1103/PhysRevB.82.155443.

[60] S. Imre and F. Balazs, *Quantum Computing and Communications: An Engineering Approach*. Hoboken, NJ, USA: Wiley, 2005.

[61] R. J. Glauber, "The quantum theory of optical coherence," *Phys. Rev.*, vol. 130, no. 6, pp. 2529–2539, Jun. 1963.

[62] P. Giorda, M. Allegra, and M. G. A. Paris, "Quantum discord for Gaussian states with non-Gaussian measurements," *Phys. Rev. A, Gen. Phys.*, vol. 86, no. 5, p. 052328, Nov. 2012, doi: 10.1103/PhysRevA.86.052328.

[63] Y. Miwa, J.-I. Yoshikawa, N. Iwata, M. Endo, P. Marek, R. Filip, P. van Loock, and A. Furusawa, "Exploring a new regime for processing optical qubits: Squeezing and unsqueezing single photons," *Phys. Rev. Lett.*, vol. 113, no. 1, Jul. 2014, Art. no. 013601.

[64] T. Eberle, S. Steinlechner, J. Bauchrowitz, V. Händchen, H. Vahlbruch, M. Mehmet, H. Müller-Ebhardt, and R. Schnabel, "Quantum enhancement of the zero-area Sagnac interferometer topology for gravitational wave detection," *Phys. Rev. Lett.*, vol. 104, no. 25, Jun. 2010, Art. no. 251102.

[65] S. L. Braunstein and P. van Loock, "Quantum information with continuous variables," *Rev. Mod. Phys.*, vol. 77, p. 513, Jun. 2005.

[66] U. L. Andersen, T. Gehring, C. Marquardt, and G. Leuchs, "30 years of squeezed light generation," *Phys. Scripta*, vol. 91, no. 5, May 2016, Art. no. 053001.

[67] B. Demoen, P. Vanheuverzwijn, and A. Verbeure, "Completely positive maps on the CCR-algebra," *Lett. Math. Phys.*, vol. 2, no. 2, pp. 161–166, Dec. 1977.

[68] A. S. Holevo, M. Sohma, and O. Hirota, "Capacity of quantum Gaussian channels," *Phys. Rev. A, Gen. Phys.*, vol. 59, no. 3, pp. 1820–1828, Mar. 1999.

[69] A. Holevo and R. Werner, "Evaluating capacities of bosonic Gaussian channels," *Phys. Rev. A, Gen. Phys.*, vol. 63, no. 3, Feb. 2001, Art. no. 032312.

[70] J. Eisert and M. B. Plenio, "Conditions for the local manipulation of Gaussian states," *Phys. Rev. Lett.*, vol. 89, no. 9, Aug. 2002, Art. no. 097901.

[71] G. Lindblad, "Cloning the quantum oscillator," *J. Phys. A, Math. Gen.*, vol. 33, no. 28, pp. 5059–5076, Jul. 2000.

[72] J. Eisert and M. M. Wolf, "Gaussian quantum channels," 2005, *arXiv:quant-ph/0505151*.

[73] N. Cerf, G. Leuchs, and E. Polzik, *Quantum Information With Continuous Variables of Atoms and Light*. London, U.K.: Imperial College Press, 2007.

[74] S. Weinberg, *The Quantum Theory of Fields*, vol. 2. Cambridge, U.K.: Cambridge Univ. Press, 1995.

[75] A. S. Holevo, *Statistical Structure of Quantum Theory*, vol. 67. Berlin, Germany: Springer, 2003.

[76] M. F. Huber, T. Bailey, H. Durrant-Whyte, and U. D. Hanebeck, "On entropy approximation for Gaussian mixture random vectors," in *Proc. IEEE Int. Conf. Multisensor Fusion Integr. Intell. Syst.*, Seoul, South Korea, Aug. 2008, pp. 181–188.

[77] D. Reynolds, "Gaussian mixture models," in *Encyclopedia of Biometrics*. Boston, MA, USA: Springer, 2015.

[78] V. Maz'ya and G. Schmidt, "On approximate approximations using Gaussian kernels," *IMA J. Numer. Anal.*, vol. 16, no. 1, pp. 13–29, Jan. 1996.

[79] V. Maz'ya and G. Schmidt, "On approximate approximations using Gaussian kernels," *IMA J. Numer. Anal.*, vol. 16, no. 1, pp. 13–29, Jan. 1996, doi: 10.1093/imanum/16.1.13.

[80] L. Gyongyosi and S. Imre, "Low-dimensional reconciliation for continuous-variable quantum key distribution," *Appl. Sci.*, vol. 8, no. 1, p. 87, Jan. 2018.

[81] G. F. Knoll, *Radiation Detection and Measurement*. Hoboken, NJ, USA: Wiley, 2010.

[82] S. S. Haykin, *Communication Systems*, 4th ed. New York, NY, USA: Wiley, 2001.

ANSHU MUKHERJEE (Member, IEEE) received the B.Tech. degree in information and telecommunication engineering from the SRM Institute of Science and Technology, Chennai, India, in 2018, and the Ph.D. degree from University College Dublin (UCD), Ireland, in 2023. He is currently an Assistant Professor with the School of Electrical and Electronic Engineering, UCD. Venturing further into academia, he pursued research with the esteemed Indian Institute of Technology (IIT) Patna. His research interests include wireless security, physical layer security, energy efficiency, and the application of optimization and machine learning in wireless communication, with a keen interest in quantum communication.

AVISHEK NAG (Senior Member, IEEE) received the B.E. degree (Hons.) from Jadavpur University, Kolkata, India, in 2005, the M.Tech. degree from the Indian Institute of Technology, Kharagpur, India, in 2007, and the Ph.D. degree from the University of California at Davis, in 2012. He is currently an Assistant Professor with the School of Computer Science, University College Dublin, Ireland. He was a Research Associate with the CONNECT Centre for Future Networks and Communication, Trinity College Dublin, before joining University College Dublin. His research interests include cross-layer optimization in wired and wireless networks, network reliability, mathematics of networks (optimization and graph theory), network virtualization, software-defined networks, machine learning, data analytics, quantum key distribution, and the Internet of Things. He is the Outreach Lead of Ireland for the IEEE U.K., and the Ireland Blockchain Group.

MOULI CHAKRABORTY (Graduate Student Member, IEEE) received the B.Sc. degree (Hons.) in mathematics from the St. Xavier's College, Kolkata, in 2016, and the M.Sc. degree (Distinction) in mathematics from the Ramakrishna Mission Vivekananda Educational and Research Institute, India, in 2019. She is a Doctoral Researcher with Trinity College Dublin, affiliated with the Science Foundation Ireland Centre for Research Training in Advanced Networks for Sustainable Societies (SFI CRT ADVANCE). During her academic pursuits, she has contributed as a Junior Researcher with the St. Xavier's College, from 2015 to 2016, delved into postgraduate research with Jadavpur University, Kolkata, from 2016 to 2017. She was a Research Assistant with RKMVERI, from 2017 to 2019. Before her current role with Trinity College Dublin, she enriched her experience as a Visiting Researcher with the International Centre for Theoretical Sciences (ICTS), Tata Institute of Fundamental Research, Bengaluru, India. Her research portfolio spans mathematical aspects of quantum communication, quantum information processing, quantum computing, machine learning, data analytics, and the emerging field of quantum machine learning. In recognition of her work, she was honored with the IEEE Antennas and Propagation Society Graduate Fellowship Program–Quantum Technologies Initiative 2021.

SUBHASH CHANDRA (Member, IEEE) received the M.Tech. degree in physics from the Indian Institute of Technology, Kharagpur, India, in 2008, and the Ph.D. degree in physics from the Dublin Institute of Technology, in 2013. He is an Assistant Professor with the School of Natural Sciences, Trinity College Dublin, Ireland. He was a Postdoctoral Researcher with the Centre for Industrial and Engineering Optics (IEO), Dublin Institute of Technology. Then, he was a Research Fellow with the School of Engineering, before became an Assistant Professor with the School of Natural Sciences, Trinity College Dublin. His research interests span across quantum physics, optics, and computing. His research focuses on optics, quantum dots, quantum physics, plasmonic, Monte Carlo Ray tracing simulation, data analytics, and more particularly, designing light management technology for photovoltaic devices and daylighting. He is developing light management software for optimizing Luminescent Solar Devices to maximize solar energy harvesting.

● ● ●